HSRP-110

HARVARD COLLEGE OBSERVATORY

PUBLICATIONS OF THE SPACE RADIO PROJECT

GROUND FEASIBILITY TESTS OF UNITY-GAIN, HIGH-DIRECTIVITY ANTENNA

NASA Contract NSR 22-007-072

Final Report

NASA Contract NSR 22-007-072

GROUND FEASIBILITY TESTS OF UNITY-GAIN, HIGH-DIRECTIVITY ANTENNA

Final Report

January 1968

Principal Investigator: G. Richard Huguenin

Prepared by

Harvard College Observatory
60 Garden Street
Cambridge, Massachusetts

TABLE OF CONTENTS

TABLES

ILLUSTRATIONS

1.0 Introduction

This report summarizes the research accomplished under Contract NSR22-007-072 entitled "Ground Feasibility Tests of a Unity-Gain, High Directivity Antenna". This antenna system was originally considered for a Radio Astronomy Explorer satellite to provide a 10 arc-degree pencil beam over the frequency range of ~ 1 - 5 MHz (Proposal 1 July 1965).

The primary astronomical objective of such a satellite would be to obtain a series of sky surveys with approximately a 10 arc-degree angular resolution at several discrete frequencies in the range between 1 and 5 MHz. The useful directivity obtainable at long radio wavelengths from satellite-borne conventional antennas is limited by severe structural problems. A conventional antenna, to produce a 10 arc-degree pencil beam at 1 MHz, would require between 1 and 2 square miles of aperture! An unconventional antenna design was sought, therefore, which could provide sufficient directivity and still pose no difficult structural problems on an Explorer-sized spacecraft.

The antenna concept studied obviates the need for a multiple wavelength structure by taking full advantage of the high signal-to-noise ratio inherent with a high sky brightness temperature relative to the ambient "room temperature". The results of the ground tests of this concept were somewhat disappointing, although the concept proved basically sound. The feasibility tests demonstrated that the system can provide at least a 10 arc-degree pencil beam with low-sidelobes for signal-to-background (S/B) ratios greater than unity. For these high S/B ratios, the antenna system fully met expectations. As the signal-to-background ratio became less than unity, the beam slowly degenerated. The processed beam, however, was always narrower than the signal beam. It was concluded that the primary cause of the beam degeneration was the non-ideal nature of the solid-state devices employed (transistors used as diodes) in the 6-U gates. It is the opinion of these investigators that a more careful selection of existing devices or the development of a special solid-state device can greatly improve the operation at low signal-to-background ratios.

In conclusion, the feasibility tests of the processing scheme demonstrate its validity at high signal-to-background ratios. The degeneration of the beam at low S/B ratios is believed to be due to mismatched diodes, a situation that probably could be corrected. The original aim of the system - to map the cosmic noise background - cannot be met with the present system. Aperture synthesis systems, however, are better suited to map the background because of higher angular resolution. However, aperture synthesis systems cannot be used for observations of the intense but time-varying sources within the solar system. The processing system studied can provide at least 10 arc-degrees for observing intense and sporadic solar system sources and therefore is complimentary to aperture synthesis systems.

2.0 System Description

In order to evaluate the usefulness of the gate-processing antenna system for long-wavelength radio astronomy, a 4-element array was designed and built to be tested using several astronomical sources of radio noise. The system which was evolved is shown in block diagram form in Figure 2-1.

A conventional array of 64 elements was also designed and built, at no cost to this contract, for comparison with the processed pencil beam. The 64-element array produces a 10 arc-degree pencil beam, the design goal of the 4-element processing array.

A boom-supported pattern transmitter was designed and constructed to facilitate adjustment of the processing receivers and to make pattern measurements on the finished instrument. The pattern transmitter utilizes either a loop or linear dipole to transmit a crystal-controlled single frequency wave, or wide-band noise at high or low power. The mode of transmission can be selected from the ground by a radio command link.

2.1 System Operation

The four dipoles and their images are used in conjunction with the three hybrids to form the three antenna patterns required. The three pattern outputs are amplified in identical, low-noise, phase-locked superheterodyne receivers. The 50 kHz IF outputs of the three 22 MHz receivers are then processed through the beam-forming gates. The receiver outputs are also square-law detected, amplified, and fed out to be recorded.

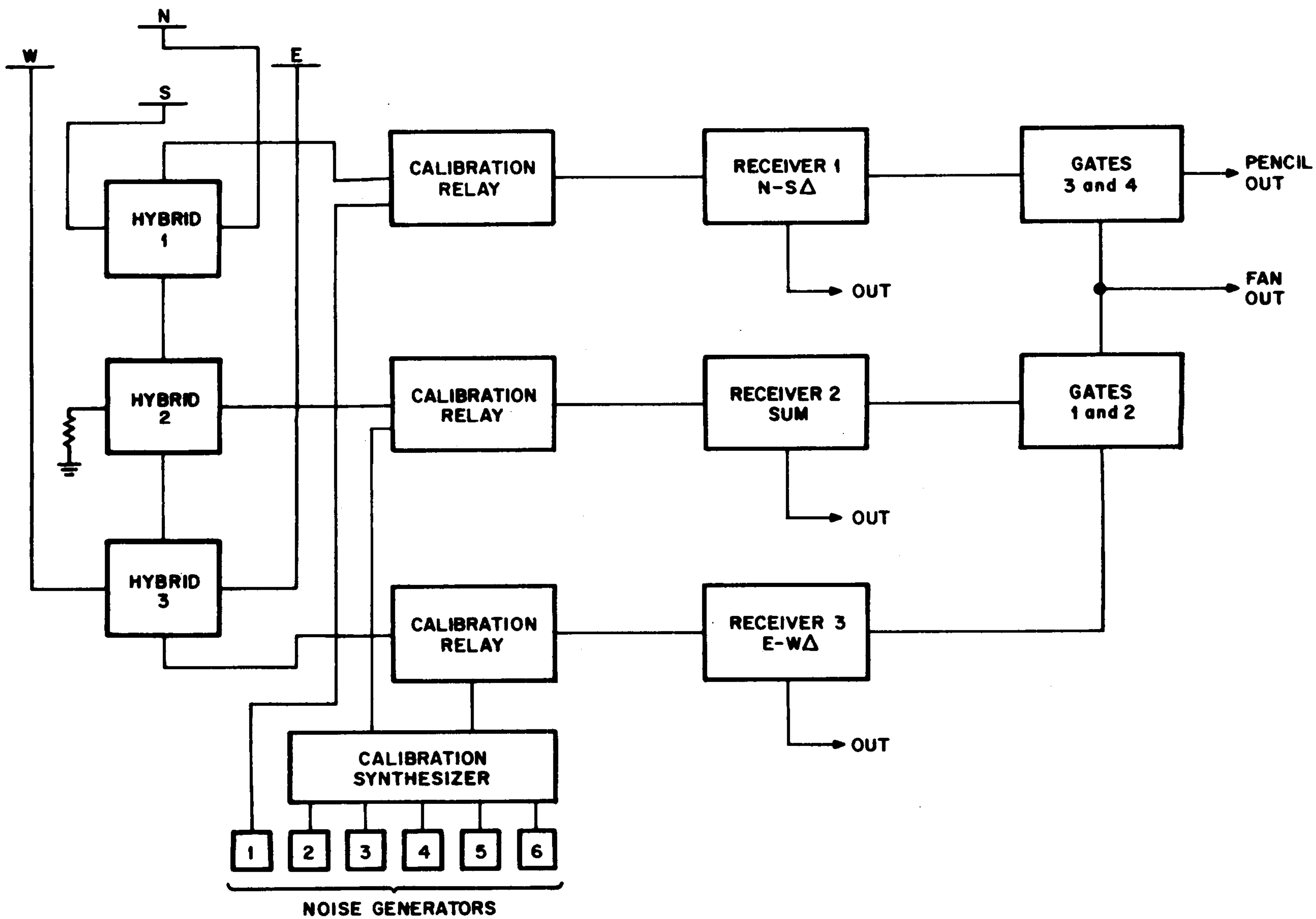

Figure 2-1 Block Diagram of System

The outputs of the first pair of gates (fan beam) and the second pair of gates (pencil beam) are also detected and recorded.

The data recording system consists of a Dymec data acquisition system and a Sanborn six channel chart recorder. The data acquisition system scans periodically through the monitored points listed in Table 2-1 and also records the time (EST) of each reading. The output medium is printed paper tape.

Calibration of the beam-forming electronics is accomplished using six specially designed solid state noise generators and a specially designed fan-beam synthesizer. A system programmer, controlled by the data acquisition system clock, controls the calibration cycle in a preprogrammed sequence.

The operator's view of the system is shown in Figure 2-2. The system's operation can be functionally understood with the aid of Figure 2-3. Consider first the generation of a fan beam. The signal input is shown schematically as resulting from an antenna gain response pattern with a maximum near the zenith. The output response of the "signal" antenna for a source in some arbitrary direction is defined as the phase reference and will be considered positive. The output response of the "reference" antenna as described in Section 2.2 for a source in the right-hand quadrant is in phase with the "signal" antenna and, for a source in the left-hand quadrant, is 180° out-of-phase. The amplified output of the "signal" antenna is fed into gate 1 as is the amplified output of the "reference" antenna as shown in Figure 2-3. The gate functions to exclude, in a non-

Table 2-1

Scanner Channel	Function
1	64-element Ryle-Vonberg radiometer output
2	4-element 10° pencil beam
3	4-element 10° fan beam
4	4-element Sum (Σ) pattern
5	4-element East-West difference (Δ) pattern
6	4-element North-South difference (Δ) pattern
7	Noise Generator #1
8	Noise Generator #2
9	Noise Generator #3
10	Noise Generator #4
11	Noise Generator #5
12	Noise Generator #6

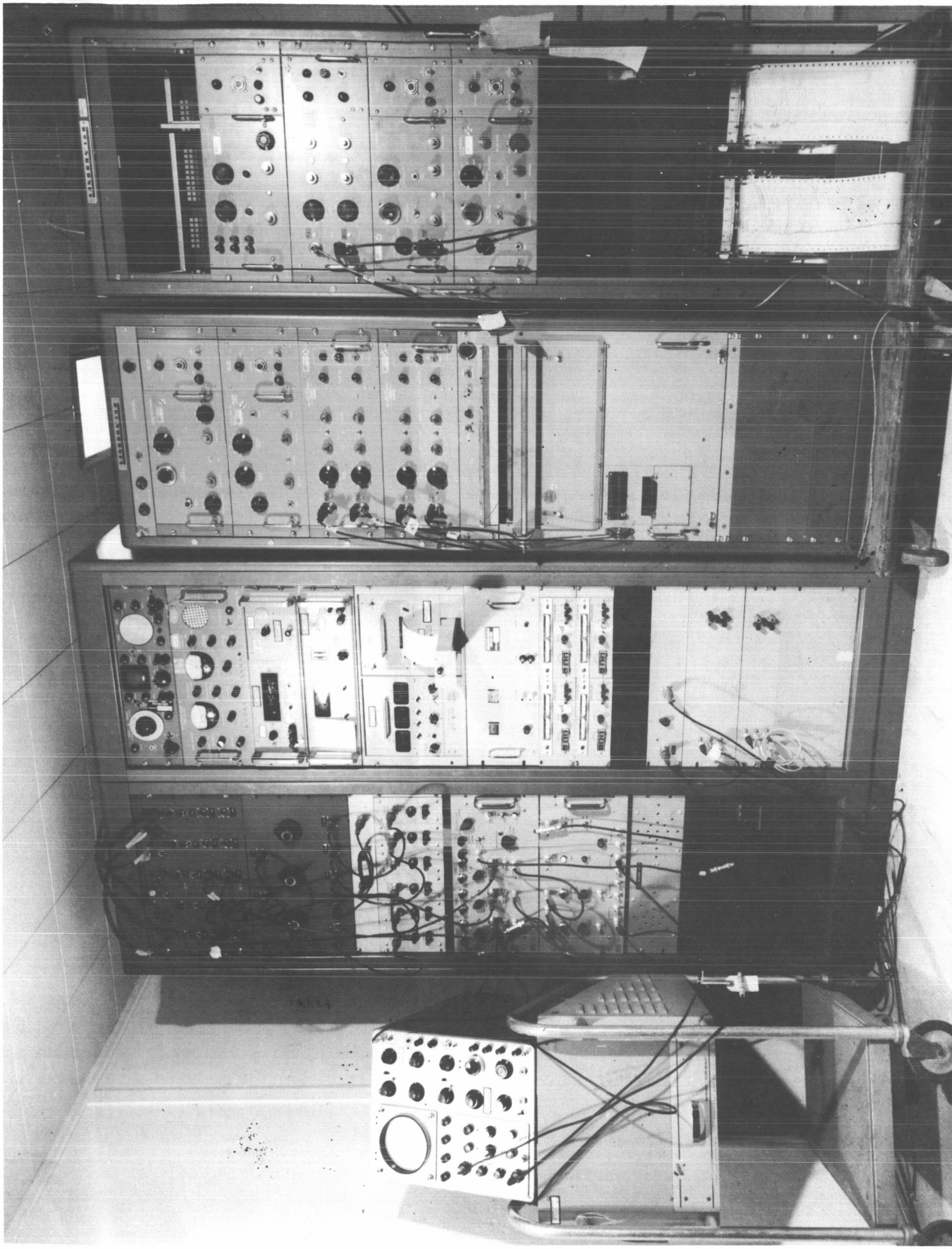

Figure 2-2 Operator's View of System

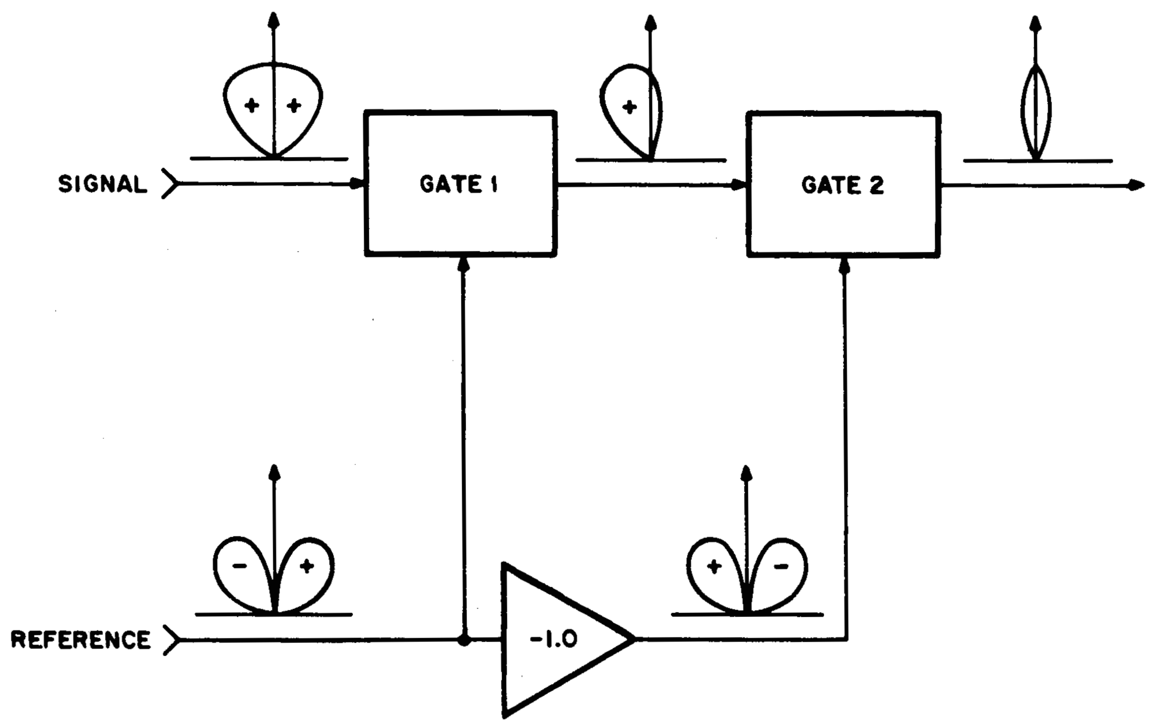

Figure 2-3 Simplified System Function

linear fashion, signals in phase with the reference. Thus, signals resulting from sources which appear outside the null in the reference are highly attenuated by the gate, whereas those appearing in the null are attenuated very little and those in the zero of the null are passed unattenuated. The gain in the reference channel determines the beamwidth by establishing the depth into the null for a source to be attenuated 3 db below the signal from a source in the null minimum.

In order to process the signals in the "left-hand" quadrant, the signal channel is passed into a second gate which is fed the same reference inverted in phase by 180°. The resulting pattern is therefore a fan beam. Utilizing a second reference antenna with a null pattern spatially oriented 90° to the first, the signal channel can be passed through two additional gates and the fan beam reduced to a pencil beam.

2.2 Antenna System

The antenna system used for the feasibility tests was analyzed theoretically by M. D. Papagiannis and the results were presented in a report entitled *A Study of Antenna Patterns for a New High Directivity Antenna Configuration* (HSRP-109). The antenna configuration used is shown in Figure 2-4 (Figure 2, MDP). The individual antenna elements were made adjustable in length and height to facilitate tuning and to allow different signal and reference patterns to be tested. A balun was mounted on each element to match the antenna into RG-8A coaxial cable of 50Ω characteristic impedance.

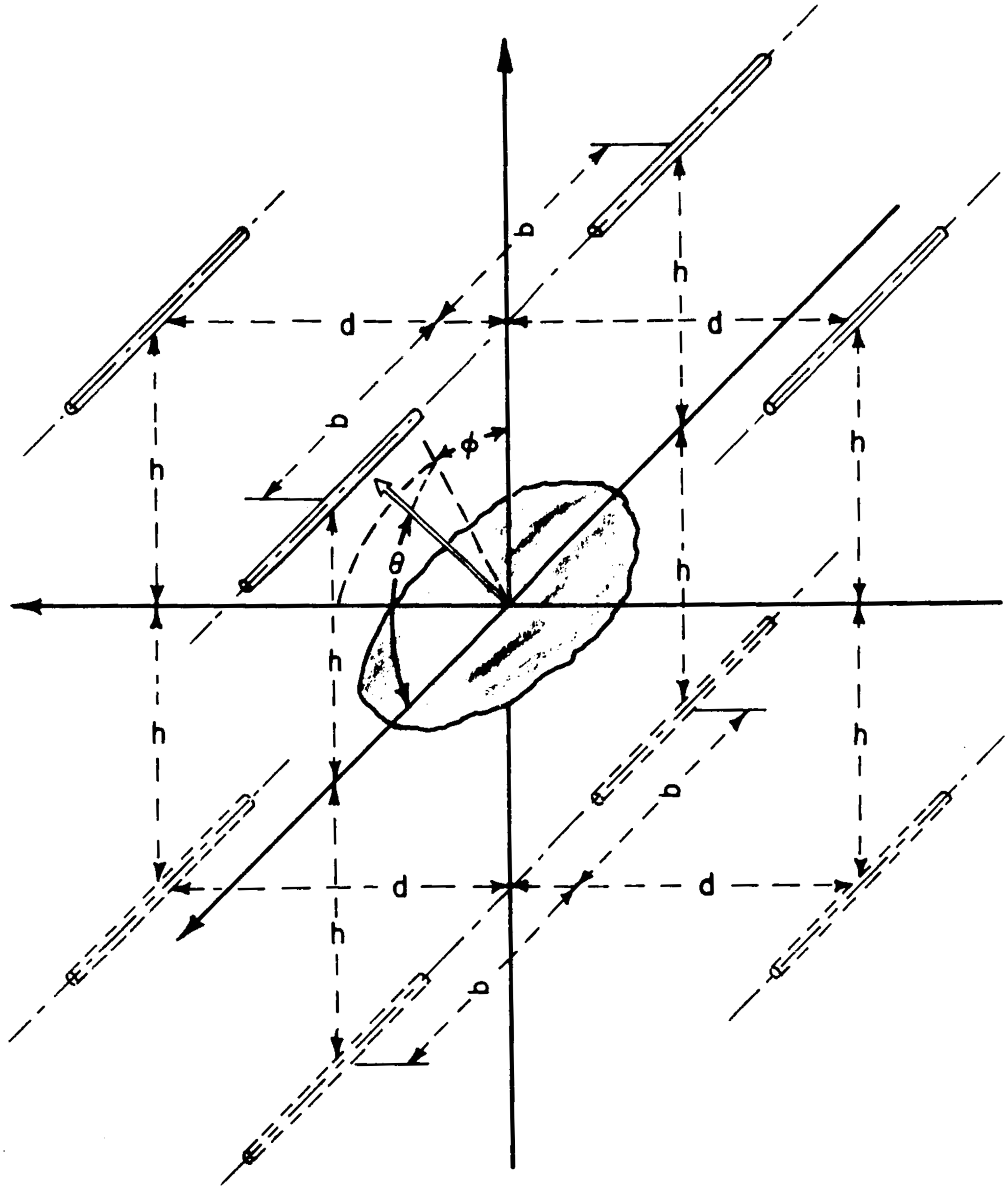

Figure 2-4 Antenna Configuration

The ground screen image plane used was 1.1 x 2.2λ in size and was fabricated of aluminum wire on 12" centers. The central 1.1 x 1.1 area was cross wired in both N-S and E-W orientations. The outer extensions on the E-W side, however, were wired only for E-W polarization.

2.3 Gate Circuits

The gate circuitry is shown in more detail in Figure 2-5. The gate circuitry processes the signal (sum pattern) waveform through four series 6-U gates with the respective reference (difference) waveforms as discussed in Section 2.1 above. Signal amplifiers were placed before and after each gate to maintain a constant signal level through the 6-U gates. To compensate for the 90° phase difference between the sum and difference patterns of the antennae, a fixed lag of 45° was placed in the first signal amplifier, and a fixed lead of 45° was placed in each reference amplifier. To insure ease of phase alignment, variable phase shifters were placed at the inputs of each reference amplifier and at the input to the first signal amplifier.

The most critical area in the detector portion of the equipment was the 6-U gate design. The main development effort was devoted toward improving the diode matching and linearizing the output of the gates. The electrical interface specifications for the gate unit are given in Table 2-2. The electrical operating characteristics are shown in Figure 3-3.

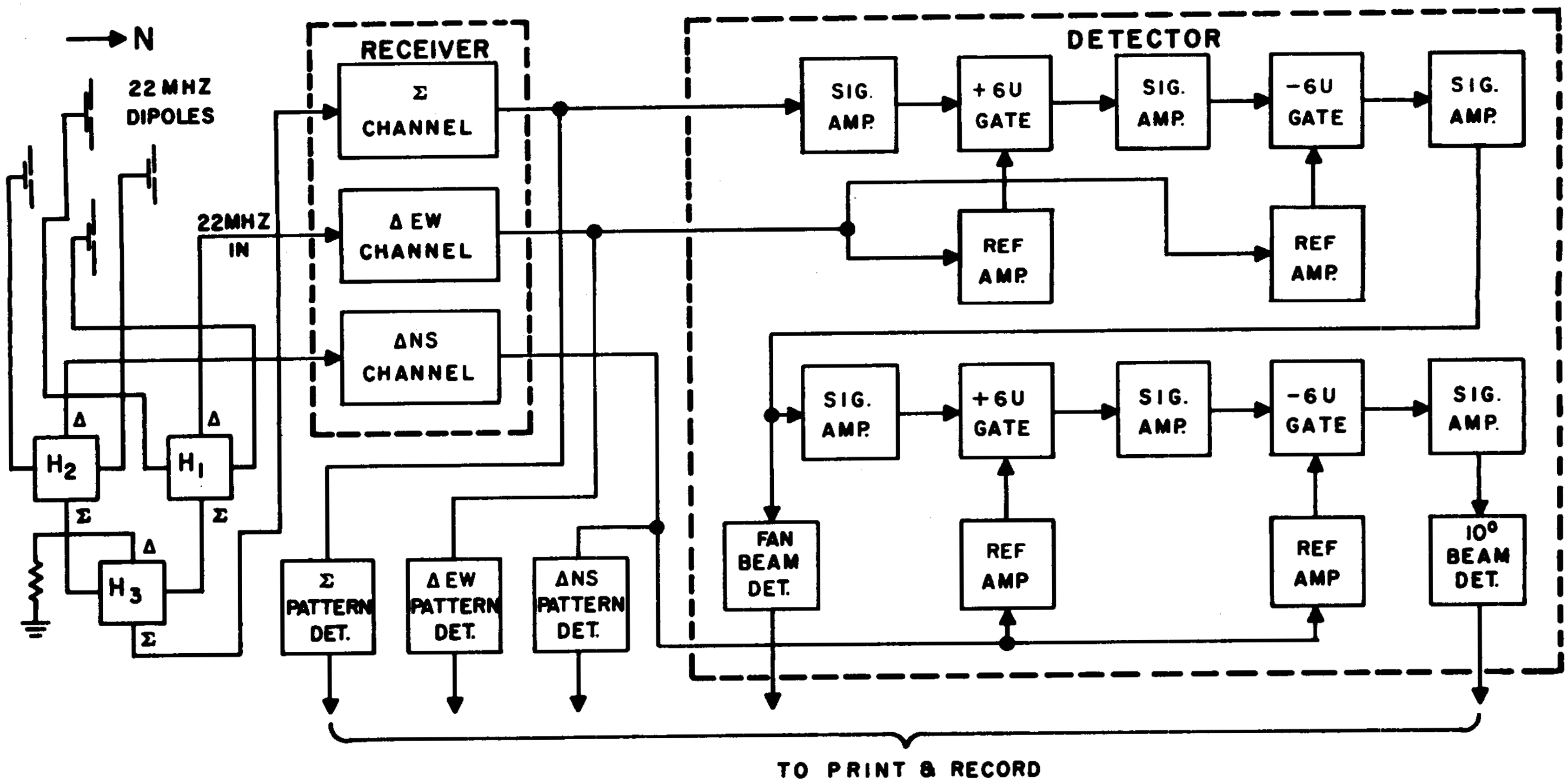

Figure 2-5 Block Diagram Beam Forming System

Table 2-2

Electrical Specifications for Gates

Detected Output:	1 v across 1 kΩ load for 80,000°K isotropic input.
Inputs:	600Ω with range of 0.015 - 3 vrms before saturation. Normal operating range of 0.3 vrms for 80,000° isotropic input.
Balance:	>50 db (60 db design goal)
Relative Phase Shift:	<0°5 electrical at gate input.
Monitor:	Phase monitor points at gate input.

2.4 Receivers

Three identical phase coherent receiver channels were required for the signal and two reference antenna patterns. The receiver specifications are summarized in Table 2-3. A block diagram is shown in Figure 2-6.

The requirement that the receiver be tunable over the frequency range of 22.000 ± 0.100 MHz with a 6 kHz bandwidth was met by incorporating a relatively wideband RF amplifier with a fixed IF and a tunable, crystal controlled first local oscillator. Triple conversion was utilized for two reasons, to ease the requirement for narrow band filtering, and to allow signal processing at the relatively low frequency of 50 kHz. The five first LO crystal frequencies are 50 kHz apart, centered at 27.505 MHz. An external local oscillator input was also provided for tuning over the complete 200 kHz range. This feature was often used to find "clear" frequencies during daytime hours. To provide phase coherence, common local oscillators for all three channels are used.

The most stringent requirement placed on the receivers was the phase tracking specification. The differential phase shift over the complete pass band of the receivers taken in pairs did not exceed two electrical degrees. The receiver noise figures were well within specification, and were some 20 db below the cosmic background.

Table 2-3

Receiver Design Specifications

Single Units

a.	Input Impedance	$50 + j0\Omega$ (adjustable for precise matching)
b.	Noise Figure:	$\leq$ 3 db
c.	Frequency Range:	22.000 ± 0.100 MHz (Tunable)
	Frequency Drift:	± 100 Hz for 60 to 90°F ambient temperature and 24 hours operation
d.	Bandwidth:	3 db - 6 kHz
		10 db - 12 kHz
		40 db - 30 kHz
	Images and All Spurious Responses:	60 db below center frequency response
e.	IF Frequency:	50 kHz
	IF Output for 80,000 °K input:	0.3 vrms
	IF Output before Clipping:	3.0 vrms (sine wave)
	IF Response:	Linear, no AGC
	IF Output Impedance:	600Ω ($\pm 10\Omega$)
f.	Detected Output for 80,000°K Input:	1 v across 1 kΩ load
	Zero Offset:	0.004 v across 1 kΩ load - input terminated
	Detected Output Response:	Square Law 1%
g.	Gain Stability:	0.2 db 60-90°F
		0.1 db 24 hrs. @ 70 ± 5°F
h.	Audio Monitor:	8Ω, 0.5 watt, gain adjustable
i.	Power Input:	110-120 VAC 60 Hz

Pairs

Phase Shift (Relative)	±0.5 electrical degrees to 3 db points
	±5 electrical degrees to 10 db points

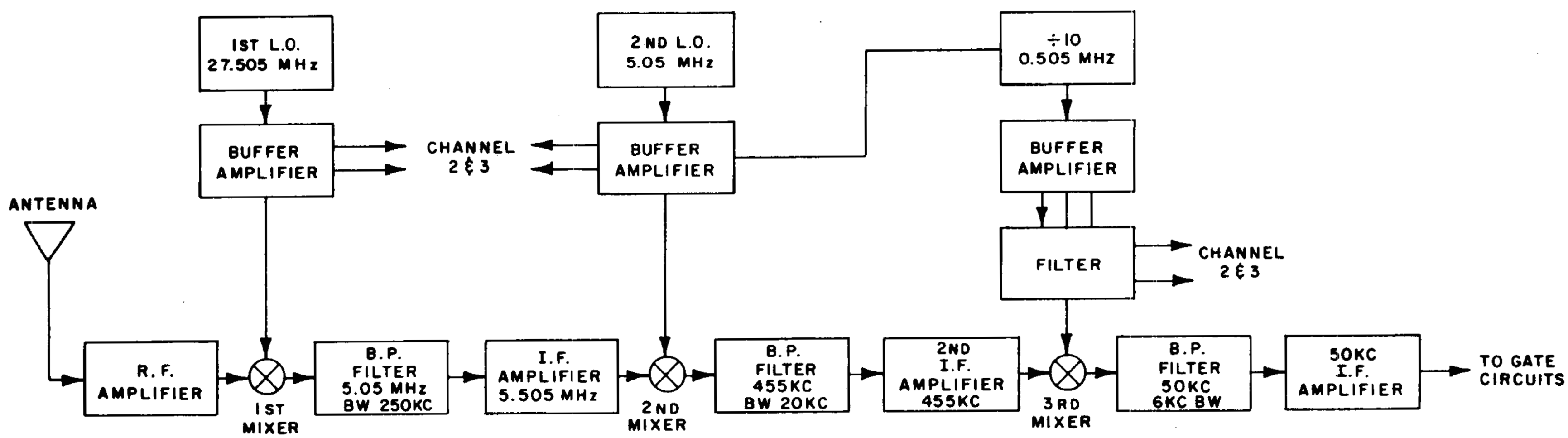

Figure 2-6 Receiver Block Diagram (Single Channel)

2.5 Calibration

The calibration of the antenna system consists of two steps: (a) an initial detailed determination of antenna properties by means of known standards; and (b) the calibration of a transfer standard to monitor periodically and correct for slowly changing parameters throughout the system lifetime.

In discussing the system used for the feasibility test in this section, we will concentrate primarily on (b) above, the development of a transfer calibration standard. Item (a) above will be discussed in Section 3.3. The transfer standard should be capable of checking system calibration from inside a spacecraft, i.e., without external probes.

The noise power density output W_o of a radio telescope operating at a given center frequency is given by:

$$W_o = G_r A_e \Omega_A \bar{b} \text{ watts Hz}^{-1} \quad (1)$$

where G_r is the receiver gain, A_e is the effective antenna-collecting area, $[m^2]$, Ω_A is the effective solid angle of the antenna beam [Sr], and $\bar{b}$ is the average sky brightness $[Wm^{-2}Hz^{-1}Sr^{-1}]$ within the beam.

The quantity to be determined by the radio telescope is the average brightness $\bar{b}$. In order to obtain the average brightness $\bar{b}$, therefore, it will be necessary to calibrate independently the beam solid angle and the product of antenna collecting area and system gain. The system calibration consists of injecting the following synthesized conditions into the receiving system through dummy antennas:

1. An isotropic sky brightness, b_o. This determines $(G_r A_e)\Omega_A$.
2. A single discrete source of flux S_o. This determines $(G_r A_e)$.
3. A single discrete source of flux S_1, S_2, etc. This determines linearity.
4. A known input noise density to determine receiver gain.

To synthesize perfectly an isotropic sky brightness would require an arbitrarily large number of noise generators. In order to test the concept within the limitations of the budget, a system utilizing only 5 independent noise generators was built. Furthermore, for a given degree of fineness N in testing, N+1 noise generators are required for the fan beam and N^2+1 for the pencil beam. Therefore the system is complete only for testing the fan beam. A block diagram of the noise generators used is shown in Figure 2-7.

The concept used for the fan beam calibration is shown in Figure 2-8. In the figure, the signal pattern (shaded) and the reference pattern (unshaded) are shown superimposed. Any sources in Region I will produce output signals (ideally) only in the signal channel. Sources in Regions II and II' will produce approximately equal amplitude signals in both the reference and the signal channels. The signal and reference outputs for sources in Region II will be in-phase and for sources in Region II' will be 180° out-of-phase. In Regions III and III' the reference output will dominate over the signal output, the two being in-phase in Region III and 180° out-of-

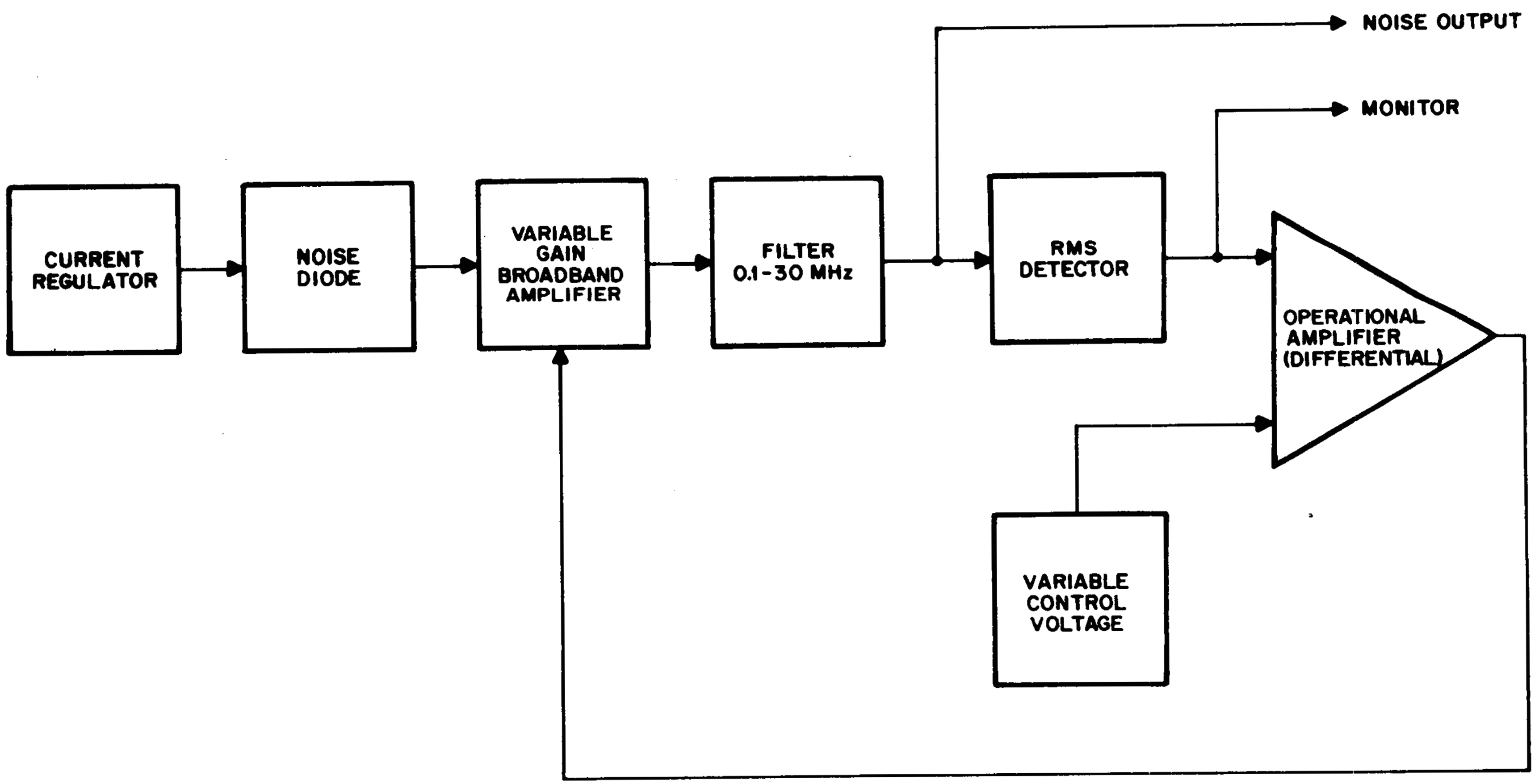

Figure 2-7 Block Diagram of a Noise Generator

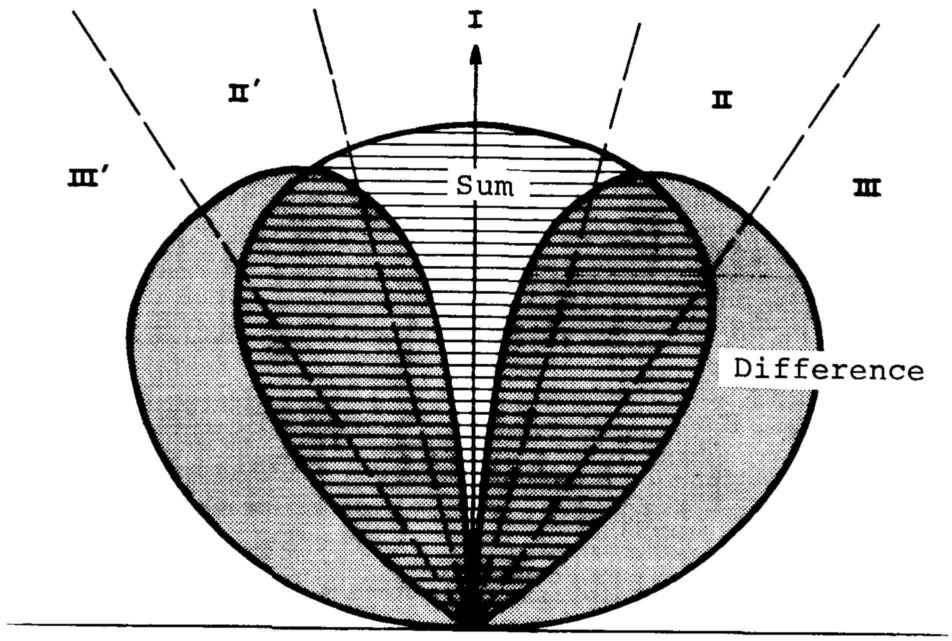

Figure 2-8 Fan Beam Calibration Concept

phase in Region III'. The breakdown into three regions is obviously a crude one, but it is felt to be indicative. Future testing undoubtedly should be for at least seven regions.

The outputs of the five independent noise generators are combined to yield a uniform sky brightness b_o. For the initial antenna setting, as shown in Figure 2-4, the spacings were as follows:

$h = \lambda/6 \ (\beta=60°)$

$d = \lambda/4 \ (\alpha=90°)$

$b = \lambda/2$

The boundaries between regions were arbitrarily defined as follows:

Region I	-10° to +10°
Region II	+10° to +30°
Region II'	-10° to -30°
Region III	+30° to +90°
Region III'	-30° to -90°

The fraction of the power density arriving in each region of the signal and reference channels for a uniform sky brightness b_o are given in Table 2-4.

Table 2-4

Relative Contributions of Pattern Regions

Region	Signal	Reference (Theoretical)	Reference (Actual)
I	.4730 (-3125 db)	.0224	0
II, II'	.1958 (-7.08 db)	.0946	.1058 (-9.76 db)
III, III'	.0677	.2196	.2196 (-6.58 db)

In practice, noise generator number 1 for Region I will not be divided between signal and reference channels, but will be split as shown in Table 2-4. The attenuators shown in Figure 2-9 for the $\alpha = 90°$, $\beta = 60°$ pattern and a brightness b of $5.44 \cdot 10^{-21}$ $w\ m^{-2}\ Hz^{-1}\ Sr^{-1}$ ($T_o = 4.0 \cdot 10^4 °K$) are:

Table 2-5
Attenuator Values

Attenuator No.	Attenuator (db)
1	8.1
2	5.1
3	22.4
4	25.2
Variable	23.9

For the same patterns, the outputs of the noise generators should be:

Table 2-6
Noise Generator Outputs

Number	Region	dbk	T	V_{mon}
1	I	107	$5.01 \cdot 10^{10}$	4.075
2	II	101.7	$1.48 \cdot 10^{10}$	1.000
3	II'	104.7	$2.95 \cdot 10^{10}$	2.325
4	III	105.2	$3.31 \cdot 10^{10}$	3.470
5	III'	105.2	$3.31 \cdot 10^{10}$	2.625
6	Ref N-S*	106	$4.00 \cdot 10^{10}$	3.050

*Through a 60 db attenuator to Receiver 3 (JD2A)

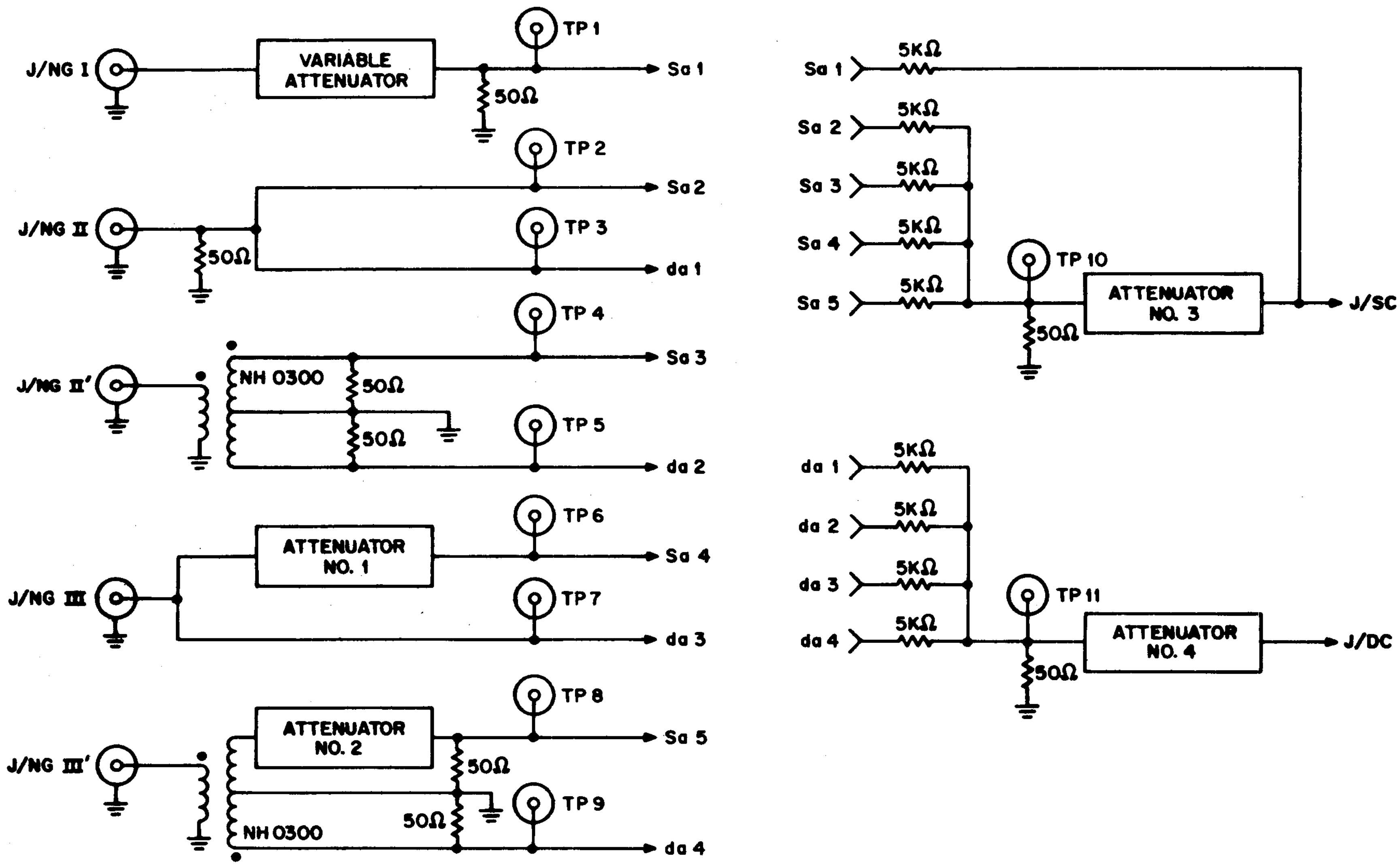

Figure 2-9 Noise Synthesizing Circuitry

The superposition of a discrete source over the uniform background is accomplished using the variable attenuator V1.

The output of NG Number 6 is inserted into the receiver Number 3 for calibration of G_R (3) only.

2.6 Pattern Measurement System

In order to measure the antenna patterns for the four-dipole, high directivity antenna configuration, a "mast and movable boom" assembly was erected to transport a small single source from ground level (0°) to zenith (90°) at any azimuth around the antenna field.

2.6.1 The Mast and Movable Boom

The mast and movable boom assembly, located at the center of the array, consists of a 50.0 foot mast mounted on a base which is 12' above ground, a boom 70.8 feet in length mounted on a movable hinge at the base of the mast, and a power winch to elevate the tip of the boom from the ground to zenith. The boom can rotate 360° around the mast and be elevated 90° in any direction by a system of ropes pulled by the power winch which has a drum 12 feet in circumference. A turns indicator is mounted on the winch to record the number of feet of rope that is wound on the drum. The pattern transmitter is mounted on a bracket at the end of the boom and is offset 86" to compensate for the offset of the boom from the mast and to compensate for any minor shifting of the mast from true vertical. Figure 2-10 shows the pattern tramsmitter attached to the boom. The mast

Figure 2-10 Pattern Transmitter Mounted on Boom

and boom assembly was one of the tasks of the Raytheon Company.

The elevation angle of the boom above the local horizon was determined using a precision theodolite in each of the four compass directions (NESW). The amount of cable wound on the drum was measured accurately (to the nearest tenth of a foot) by a turns indicator propelled by the drum of the winch. The actual angles above the ground level center of the array were calculated from the observed angle data and then they were plotted against their corresponding turns indicator readings.

For very accurate measurements the system can be calibrated to reach within ±5 arc minutes of any desired angle in a quadrant, by setting the turns counter in the carefully determined electrical zenith.

The boom calibration was checked on both dry and rainy days and it was found that rope stretch due to changes in relative humidity did not affect the angle calibration.

2.6.2 Pattern Transmitter

The pattern transmitter was used in conjunction with the mast and movable boom to make final phase adjustments and pattern measurements. The transmitter was designed to be battery operated and to provide for stable operation in an outdoor environment. It was required that the pattern transmitter be able to transmit in four modes: crystal controlled oscillator high power; crystal controlled oscillator low power; noise generator high power; and noise generator low power. Furthermore, in order to provide signals of proper polarization in the E and H planes, both a magnetic and electric dipole antenna were incorporated. The antenna selection and mode selection could be controlled from the ground by wireless remote control. A set of pilot lights on the transmitter could be commanded on by remote control to verify proper mode and antenna selection. The electrical specifications for the pattern transmitter are summarized in Table 2-7 and a block diagram is given in Figure 2-11.

Table 2-7

Pattern Transmitter Specifications

CW Mode

a.	Frequency:	22.000 ±0.100 MHz (selected by Xtal)
b.	Frequency Stability:	±0.1 kHz for ±20°F variations in range 0-100°F and supply voltage change of ±10%
c.	Power Output:	AGC'd to 0.1 db for ±20°F variations in range of 0.100°F and supply voltage change of ±10%
	Low:	To provide 0.1 μv/meter at antenna location
	High:	To provide 10μv/meter at antenna location

Noise Mode

d.	Frequency Bandwidth:	1 db: 200 kHz 3 db: 500 kHz
e.	Power Output:	AGC'd to 0.1 db for ±20°F variations in range of 0-100°F and supply voltage change of ±10%
	Low:	To provide 0.1 μv/meter at antenna location (6 kc bandwidth)
	High:	To provide 10 μv/meter at antenna location (6 kc bandwidth)
f.	Control:	Remote through radio control circuit with the following functions: (1) OFF (2) CW-HIGH (3) CW-LOW (4) NOISE-HIGH (5) NOISE-LOW
g.	Power:	Batteries - life > 12 hours before recharge
h.	Mechanical Interface: Antenna Size	Dipole 1 meter tip-tip Loop 1 meter diameter

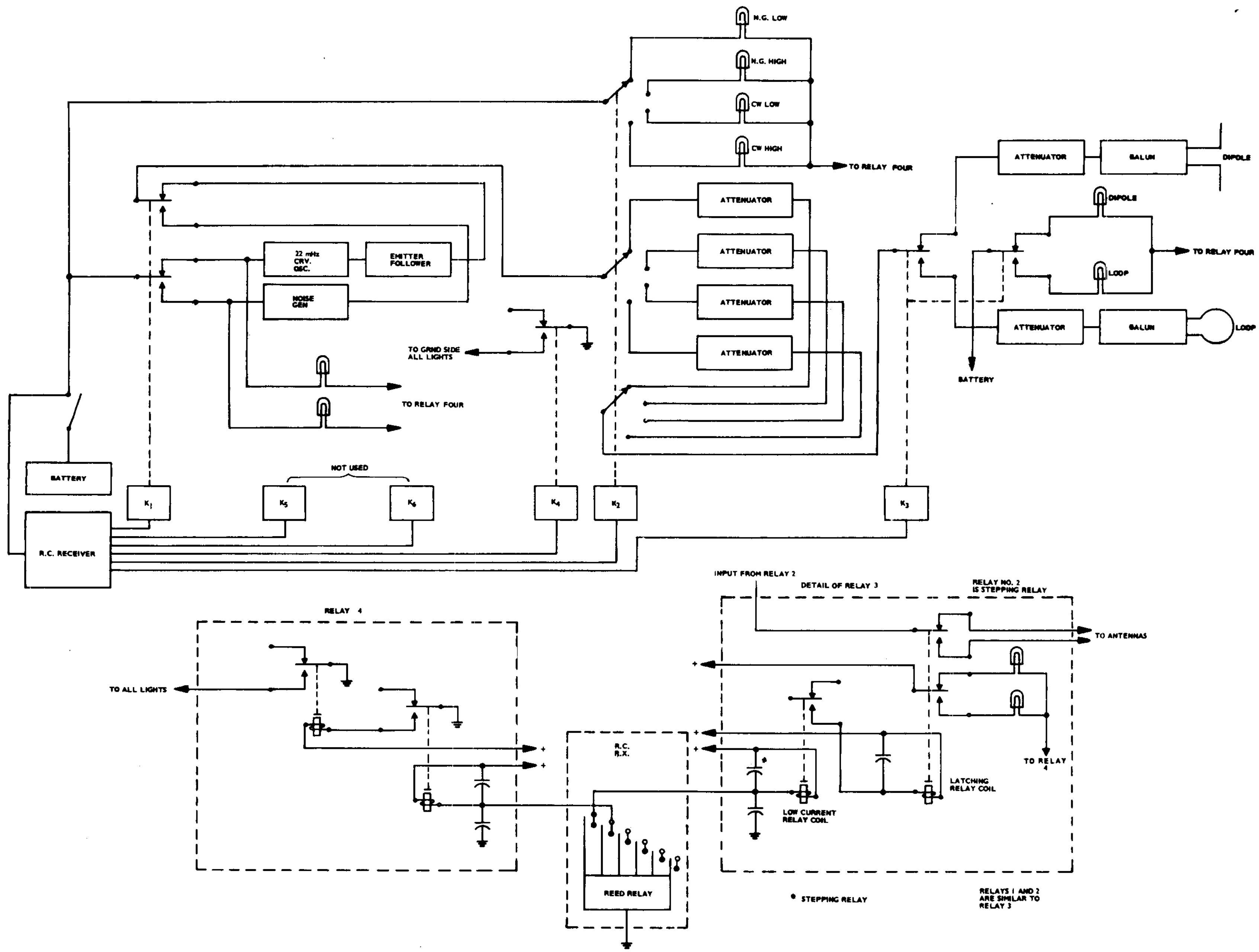

Figure 2-11 Block Diagram of Pattern Transmitter

3.0 Subsystem Tests

The individual subsystems were tested prior to their integration into the final system configuration. The end results of these continuing subsystem tests are presented in the following sections. Intermediate test results are not included.

3.1 Antenna Tests

Antenna patterns were made of both the two-element and the four-element configurations. The procedure followed was to place the pattern transmitter at the electrical zenith and adjust detector gains for maximum meter deflection. For primary antenna pattern measurements, attenuation of at least 20 db was inserted between the antennas and the receiver to suppress cosmic noise and other interfering signals and still remain within the square-law region of the receiver.

Following level adjustments, the pattern transmitter was turned off and the background level monitored. The outputs of the receiver detectors were recorded using the Dymec data acquisition system. At least five separate samples of each reading were obtained. At angles away from the main lobe response, the attenuation between the antenna and receiver was reduced to give a higher signal to noise ratio. When attenuator changes were made, measurements were overlapped and the new background level recorded.

The normalized patterns for the 2 elements (sum and difference) are shown in Figure 3-2 along with the computed patterns. The small difference between the computed and measured patterns is undoubtedly due to the sphericity of the waves from the pattern transmitter, as discussed in Section 2.6 above.

3.1.1 Antenna Impedance

The North-South pair of antennas was first installed and adjusted for the following set of parameters:

$$h = \lambda/6 \quad (\beta=60°)$$
$$d = \lambda/4 \quad (\alpha=90°)$$

The antenna impedances (series equivalent) were measured at the laboratory end of the individual transmission lines utilizing the instruments shown in Figure 3-1. During the measurement of any given antenna, the others were terminated.

The results of these preliminary measurements demonstrated that the antenna element could be tuned properly without modifying the balun transformers.

The two additional antennas were assembled, and added to the existing pair of antennas in the optimum configuration; that is, with $\alpha=kd=\pi/3$, $\beta=kh=\pi/2$, and $kb=\pi$, where $k=2\pi/\lambda$. The derivation of the optimum configuration is discussed by Papagiannis (1967). The impedance of each element of the array, measured with the remaining elements connected to the input hybrids, is listed in Table 3-1.

Table 3-1

Antenna	Impedance (22.0 MHz)
North	50.0Ω
South	48.5Ω
East	45.0Ω
West	47.0Ω

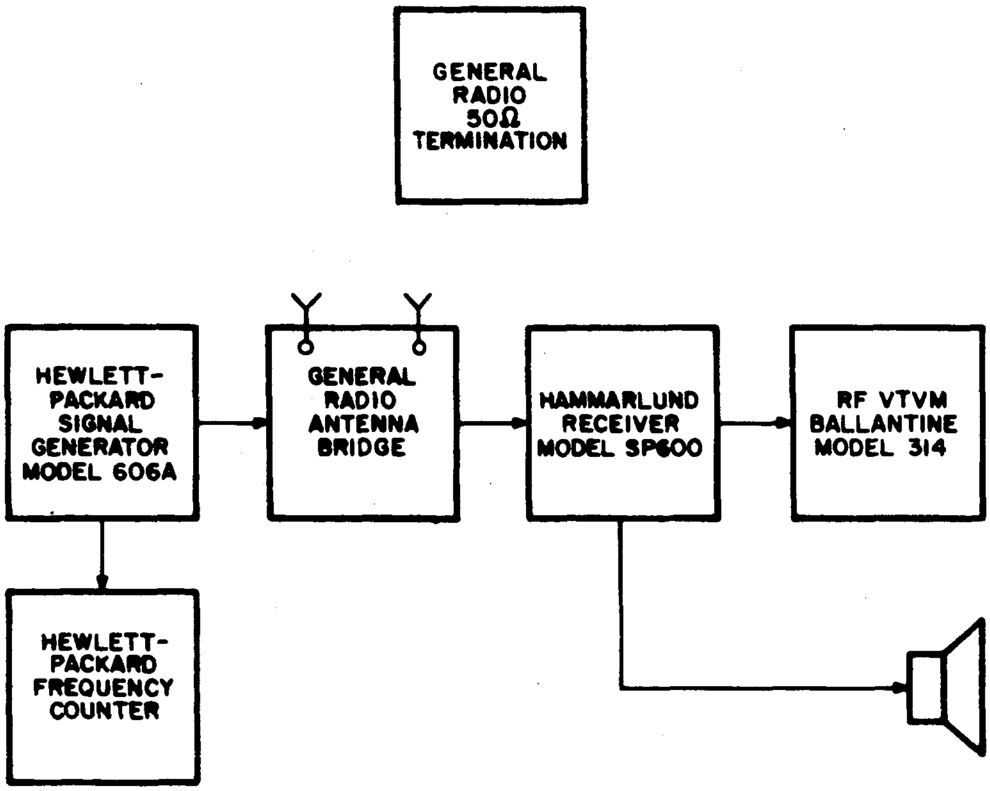

Figure 3-1 Block Diagram Antenna Impedance Measuring Equipment

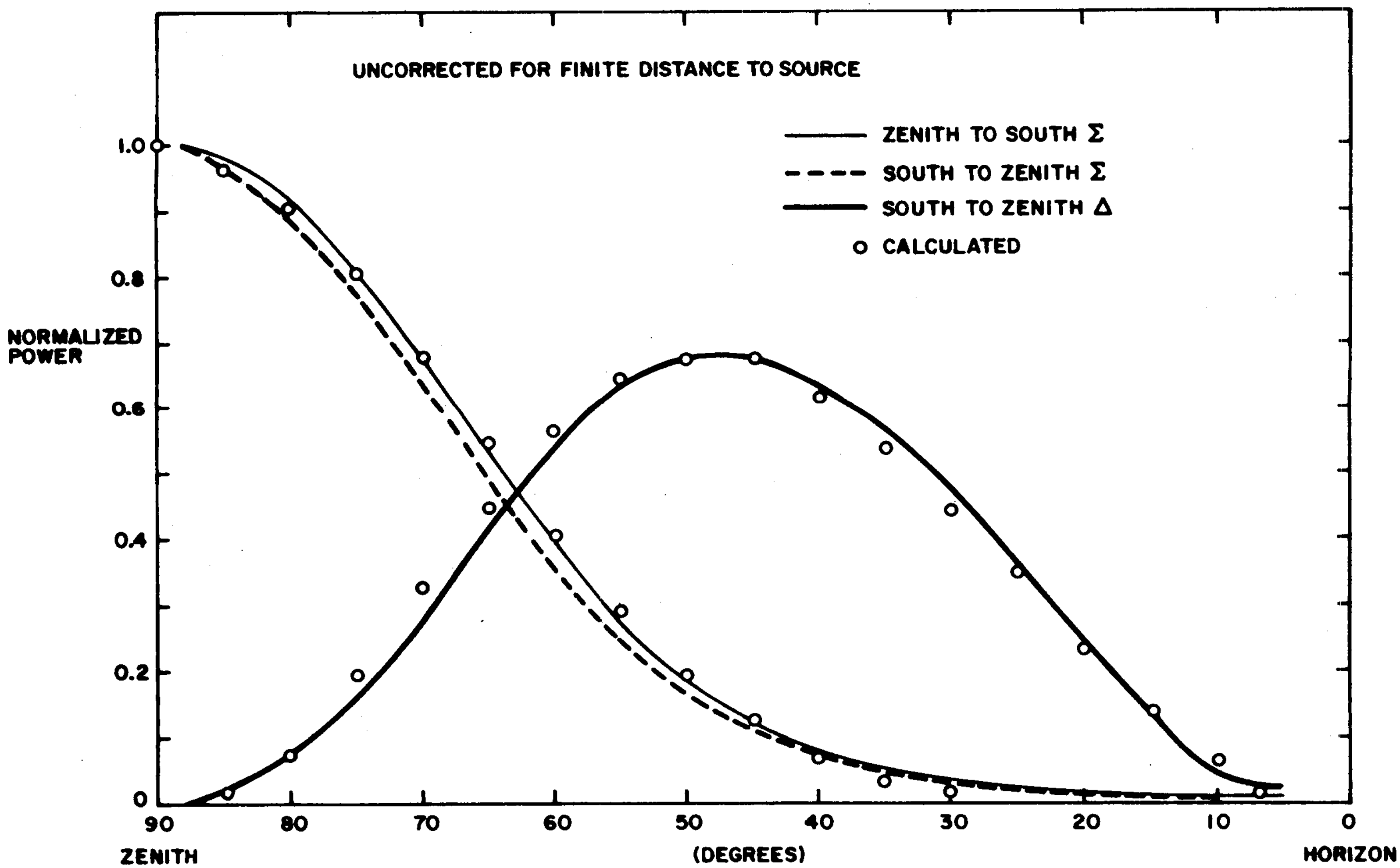

Figure 3-2 Normalized vs. Computed Antenna Patterns

The antenna impedance was re-measured periodically throughout the testing period to insure stability of the antenna structures. No significant changes were noticed after an initial problem of a shift in antenna footings was noted and corrected.

3.2 Processor Tests

The most critical area in the detector portion of the equipment was the 6-U gate design. The main effort was to improve diode match, and to linearize the output of the gates. The 6-U gate characteristics are shown in Figure 3-3. Preliminary laboratory testing of the gate circuits was somewhat limited. A single reference was used, and signal processing was through a maximum of two 6-U gates. Correlation between reference and signal was maintained by dividing power from a single source. The reference signal was fed through a resolver so that the magnitude and phase were controlled manually. One of the aspects that was tested, was noise attenuation as a function of signal level. The signal was noise in a bandwidth of 6 kHz centered at 50 kHz. Results are shown in Figure 3-4. One can readily see that optimum "out-of-beam" noise attenuation results when signal levels fall between .316 volts and 1 volt. Reference levels would then be dictated by signal levels and the beam width desired. Low "turn on" voltage and good diode matching at low levels would improve the attenuation factor for low signal levels.

During field tests, signal levels in the gate circuits were therefore set at approximately 1 volt under normal sky temperatures. Reference levels were set to approximately 3 volts

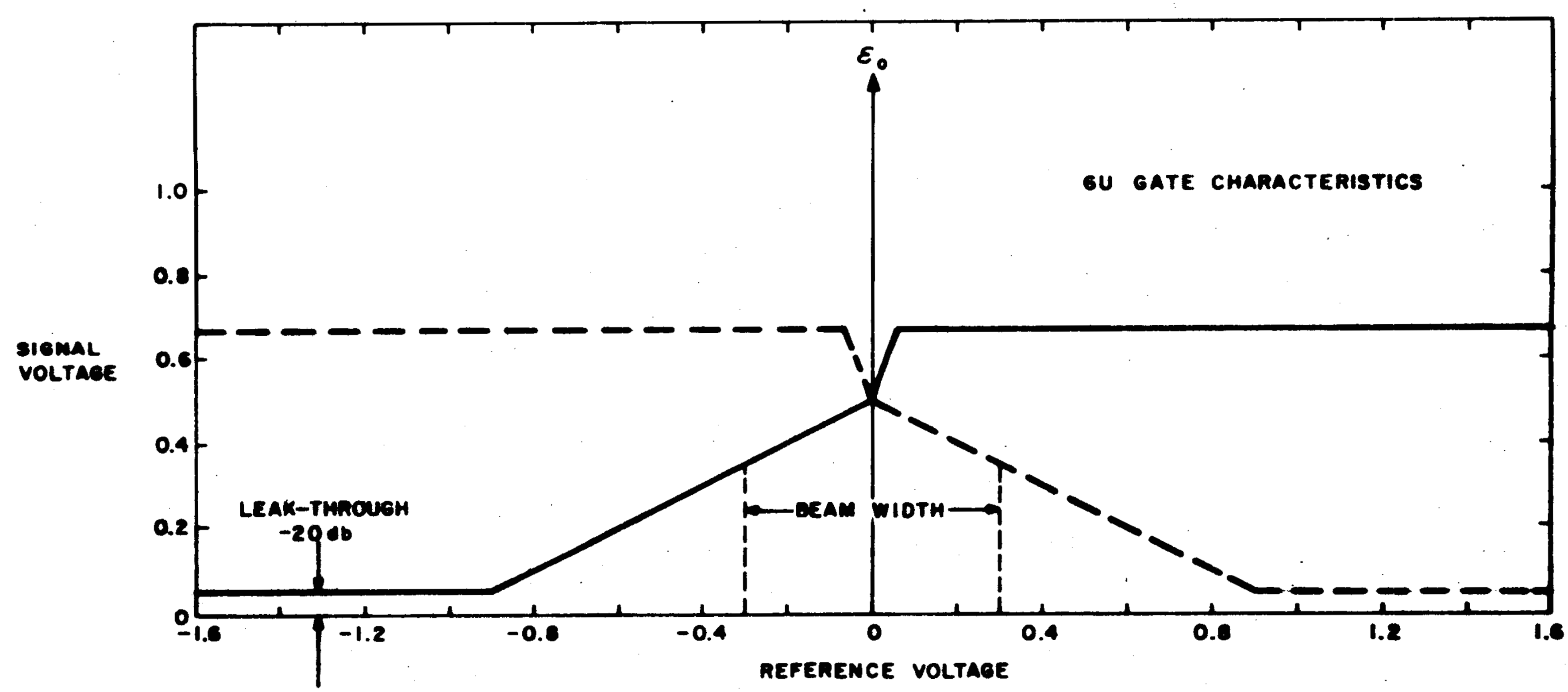

Figure 3-3 6U Gate Characteristics

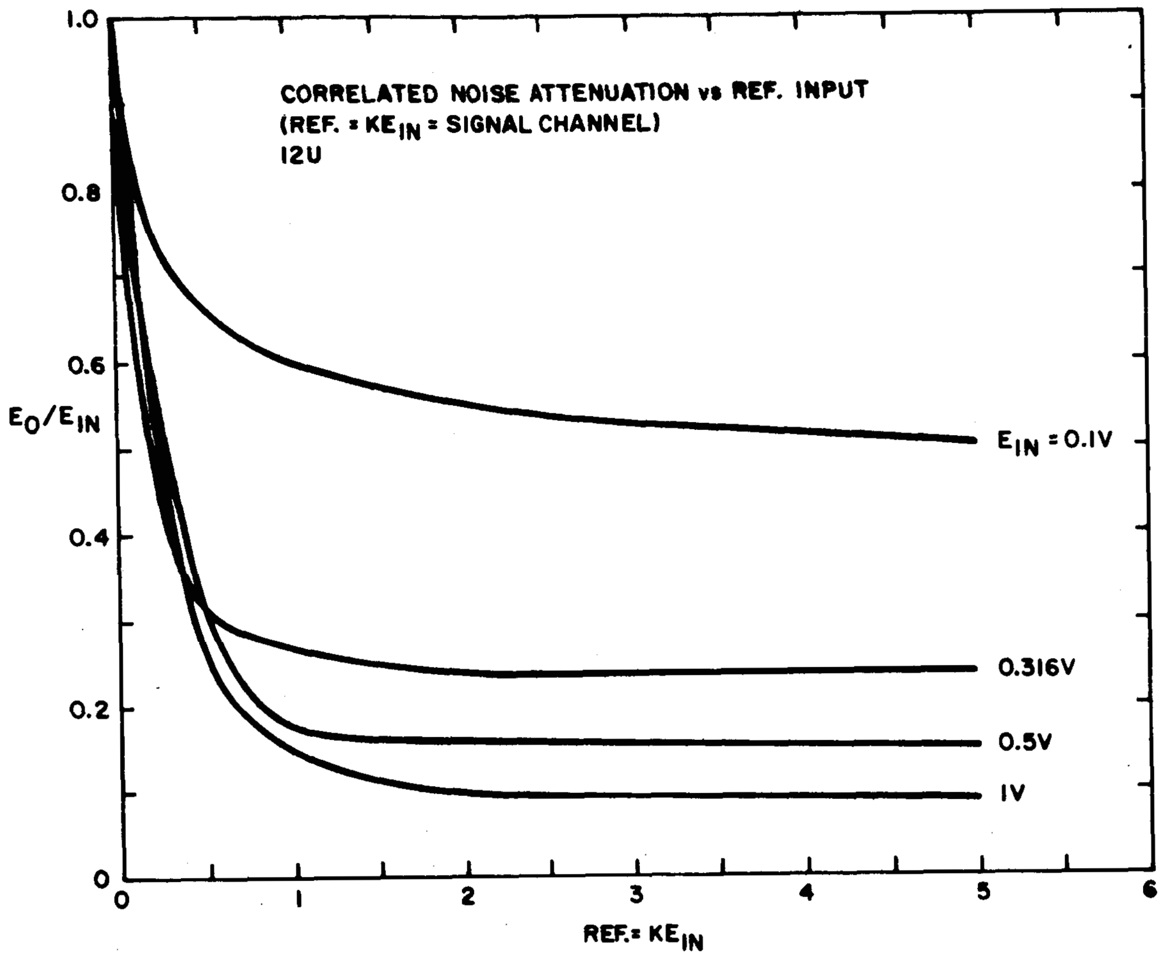

Figure 3-4 Correlated Noise Attenuation vs. Reference Input

under the same conditions. These settings were optimum and were not changed, even though the background noise varied somewhat at different times during the day.

3.2.1 Patterns

The field adjustments of the beam-forming electronics were facilitated by the ability to measure antenna patterns rapidly and repeatedly. The mast and boom assembly, with the pattern transmitter, were used continually during the tune-up period from June until mid-August. After the system was optimally adjusted, final pattern measurements were made which are presented here.

Because of the non-linearity of the system, patterns were measured at various source-to-background ratios (S/B). Patterns were also repeated using noise and continuous wave signals from the pattern transmitter. The high source-to-background ratio patterns, as made with the noise transmitter, are shown in Figure 3-5 for the East-West plane (H-plane) and in Figure 3-6 for the North-South plane (E-plane). The cosmic noise background was suppressed in determining the patterns shown in Figures 3-5 and 3-6 by inserting 20 db pads between the hybrid outputs and the receiver inputs. The noise intensity from the pattern transmitter was then adjusted to give an output deflection at zenith equal to the mean cosmic noise level in the signal (sum) pattern. The data shown in Figures 3-5 through 3-18 have been corrected for the changing distance of the pattern transmitter (< 10%), but not for the effects of a spherical wave.

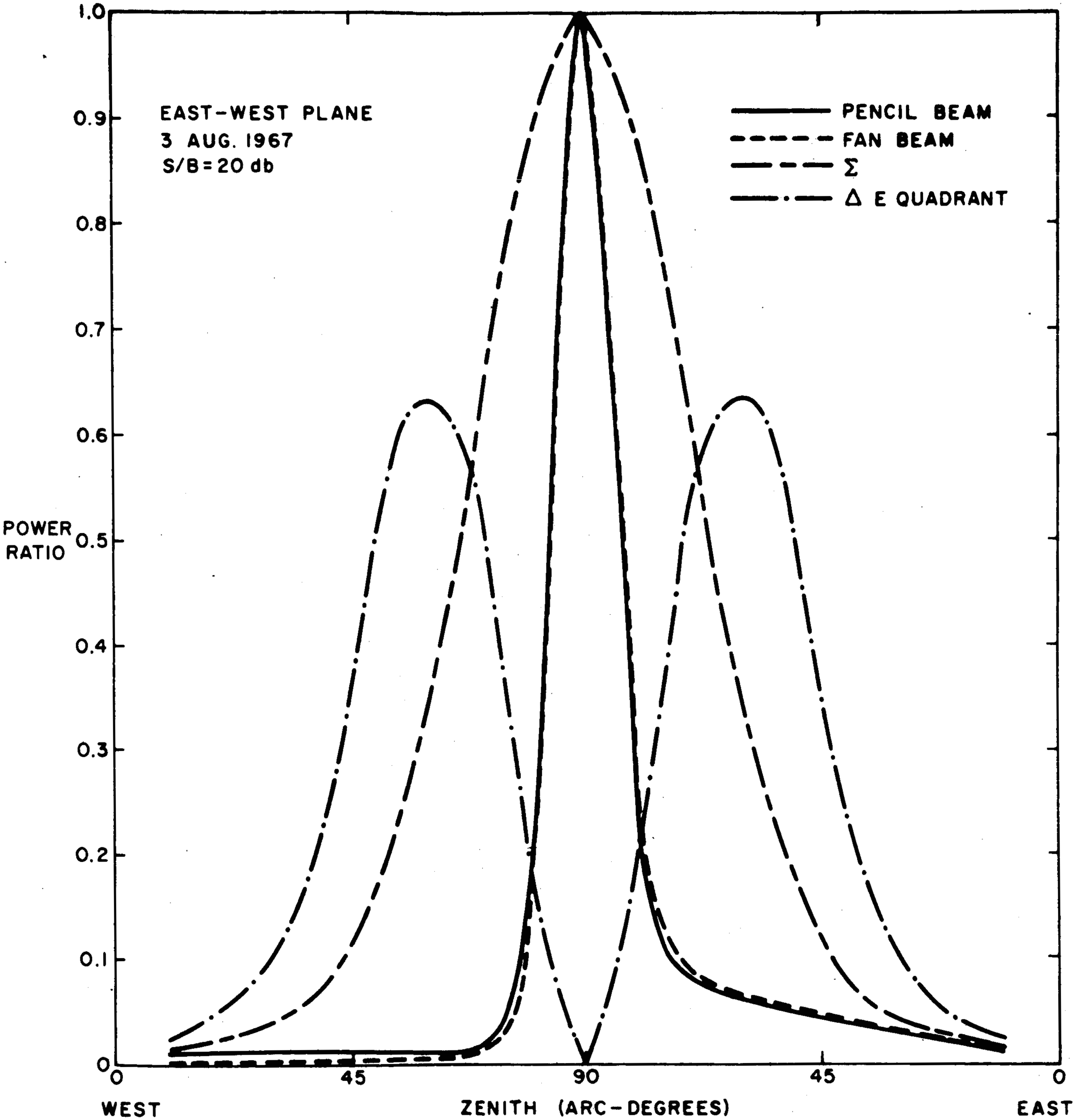

Figure 3-5 High Source-to-Background Pattern East-West Plane

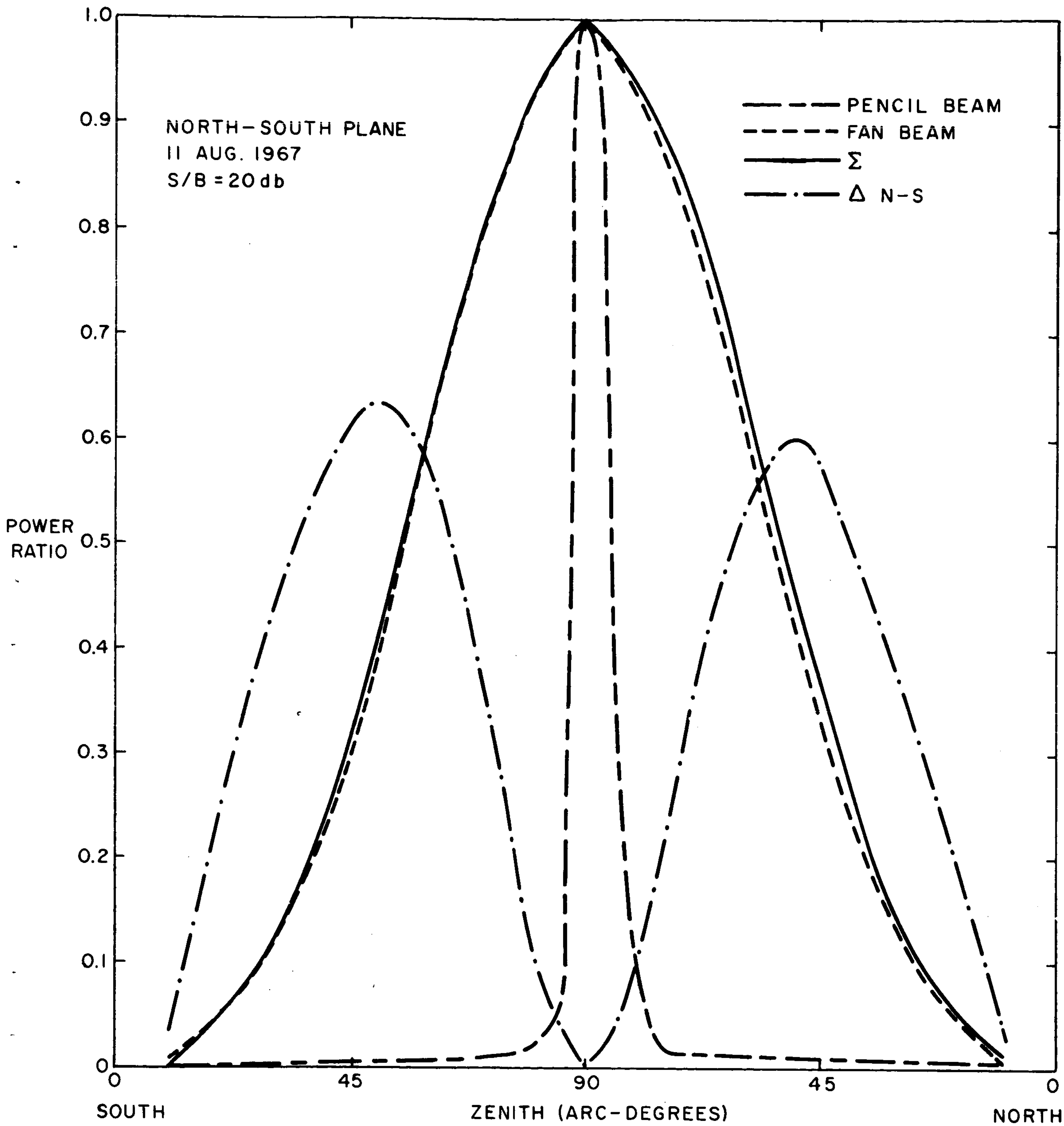

Figure 3-6 High Source-to-Background Pattern North-South Plane

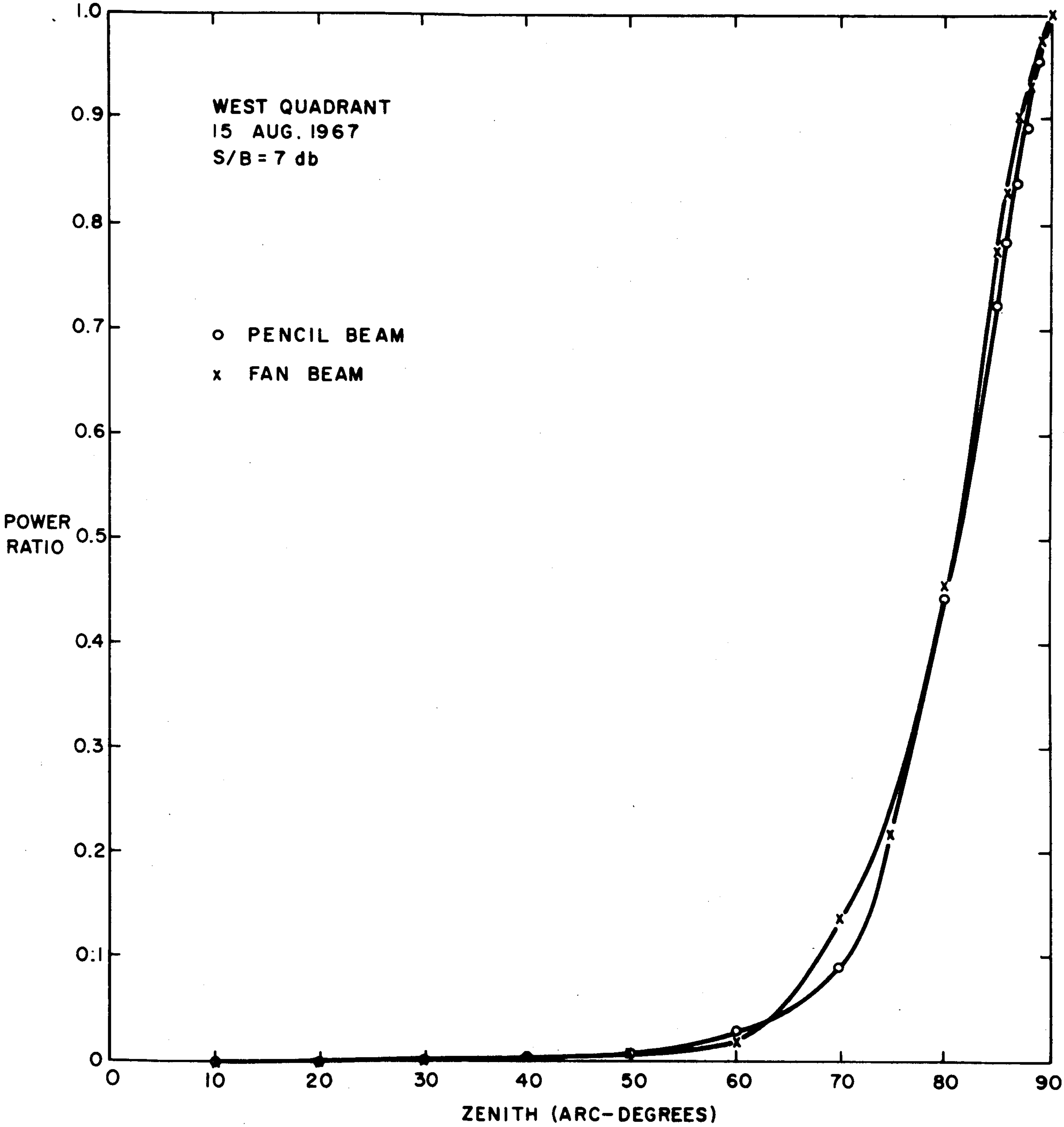

Figure 3-7 Measured Antenna Pattern

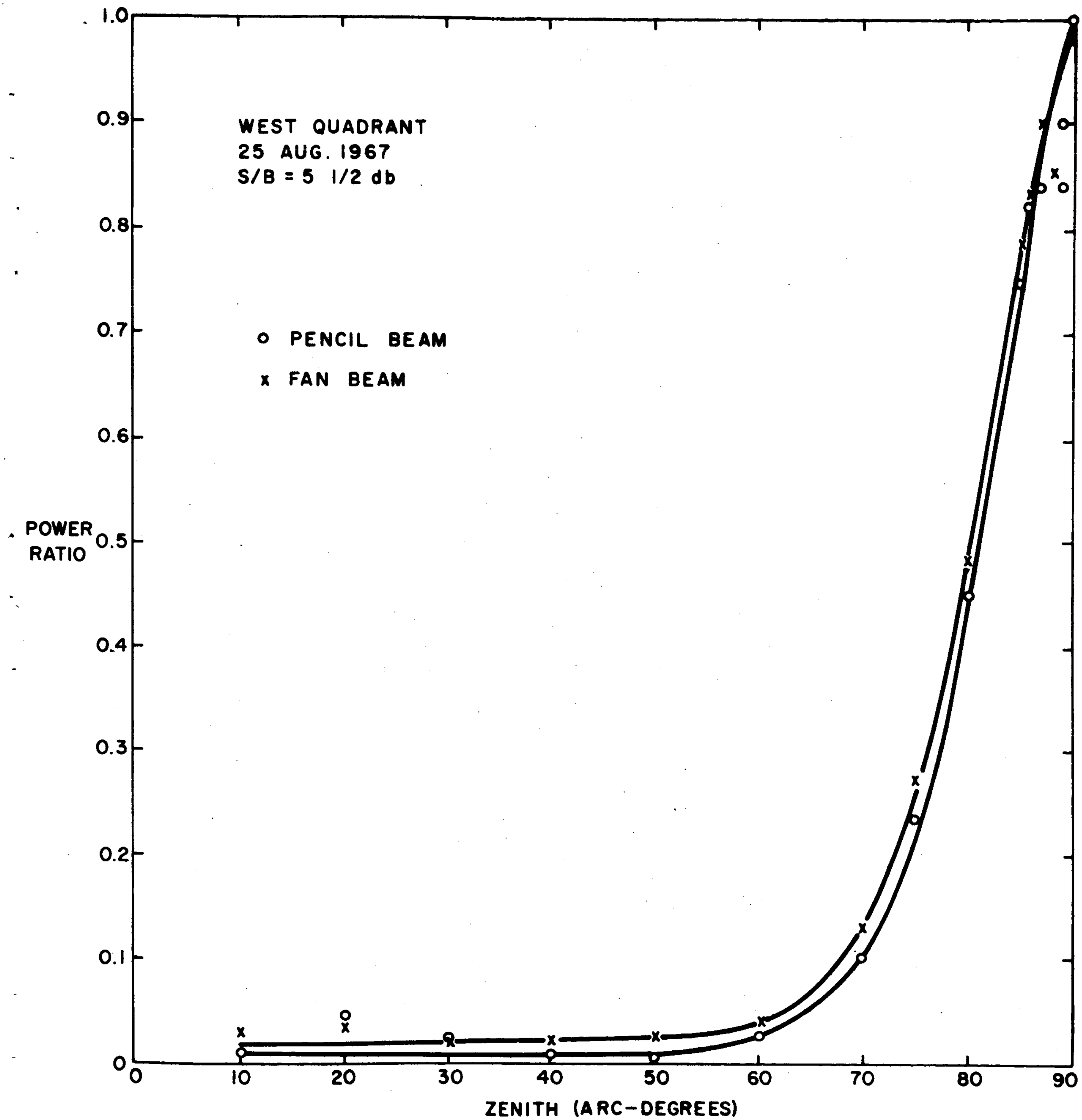

Figure 3-8 Measured Antenna Pattern

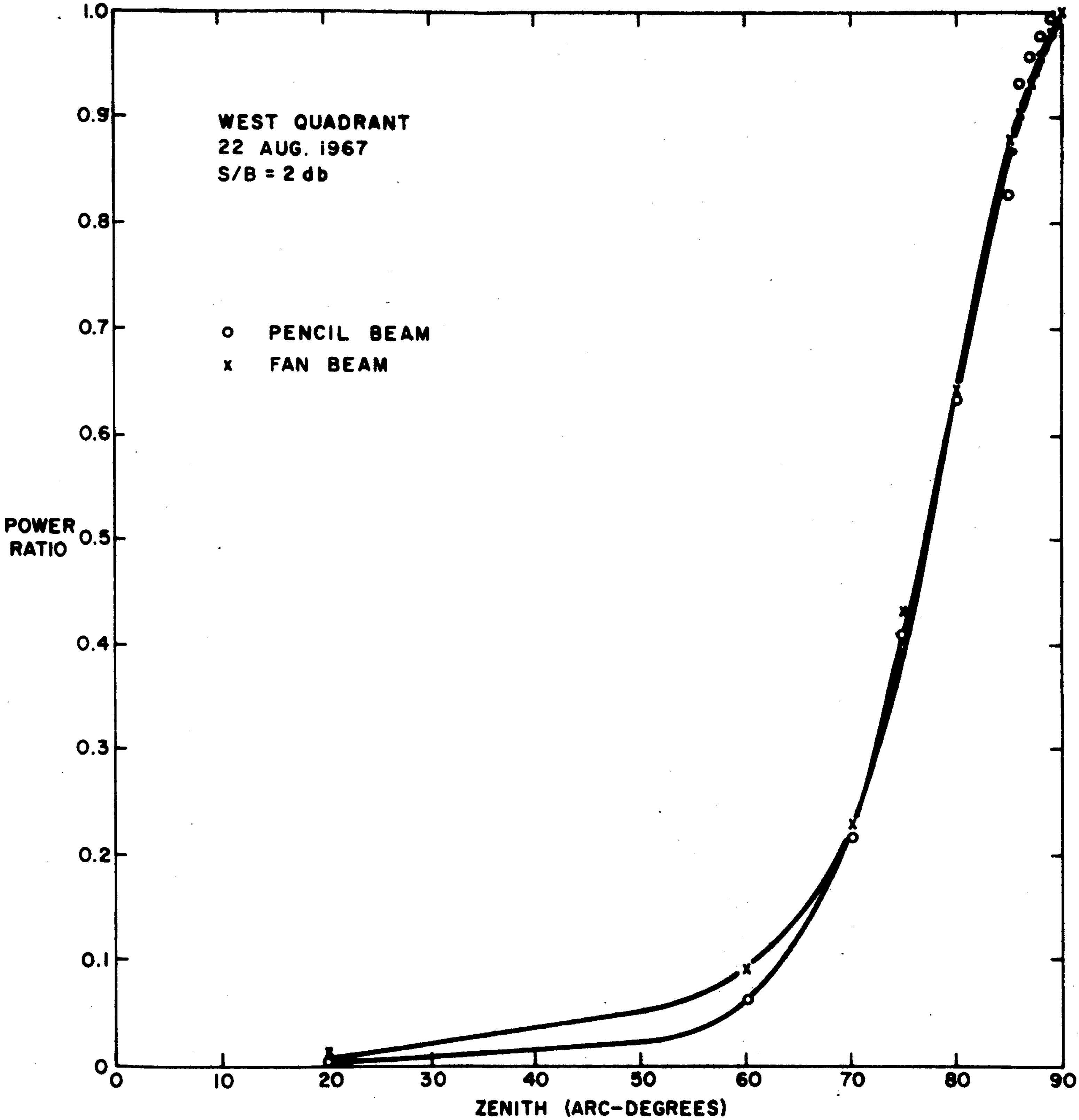

Figure 3-9 Measured Antenna Pattern

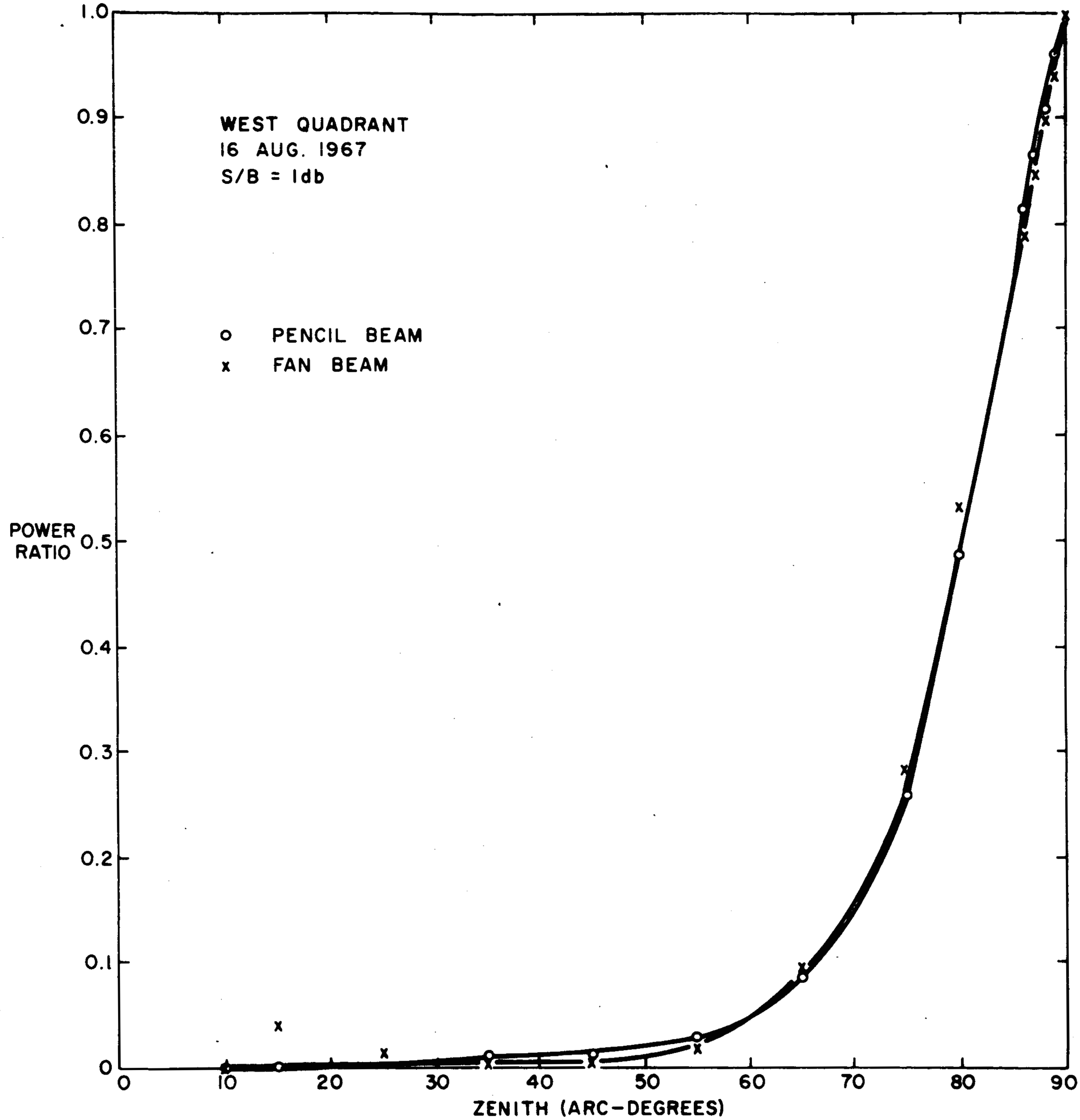

Figure 3-10 Measured Antenna Pattern

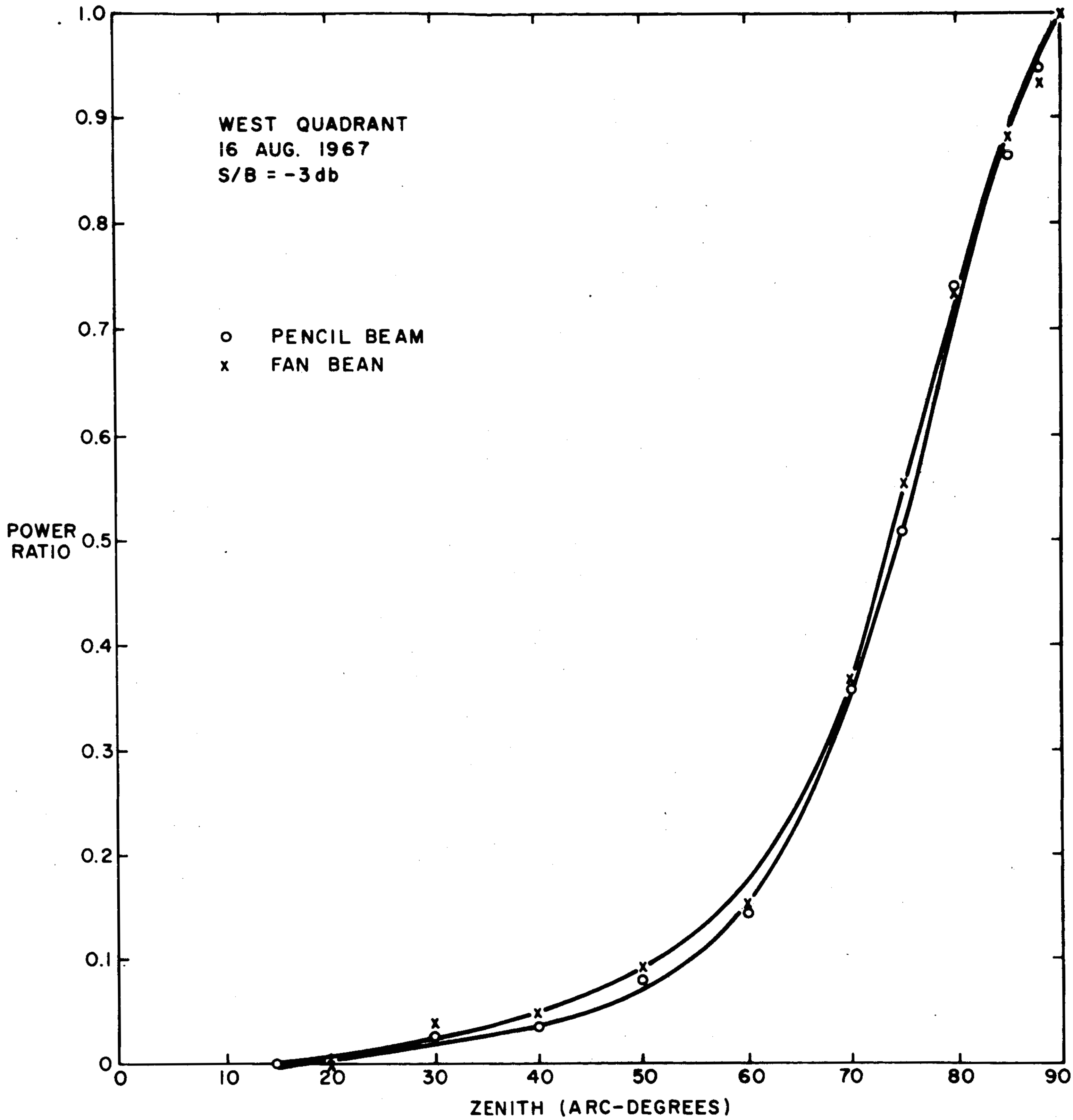

Figure 3-11 Measured Antenna Pattern

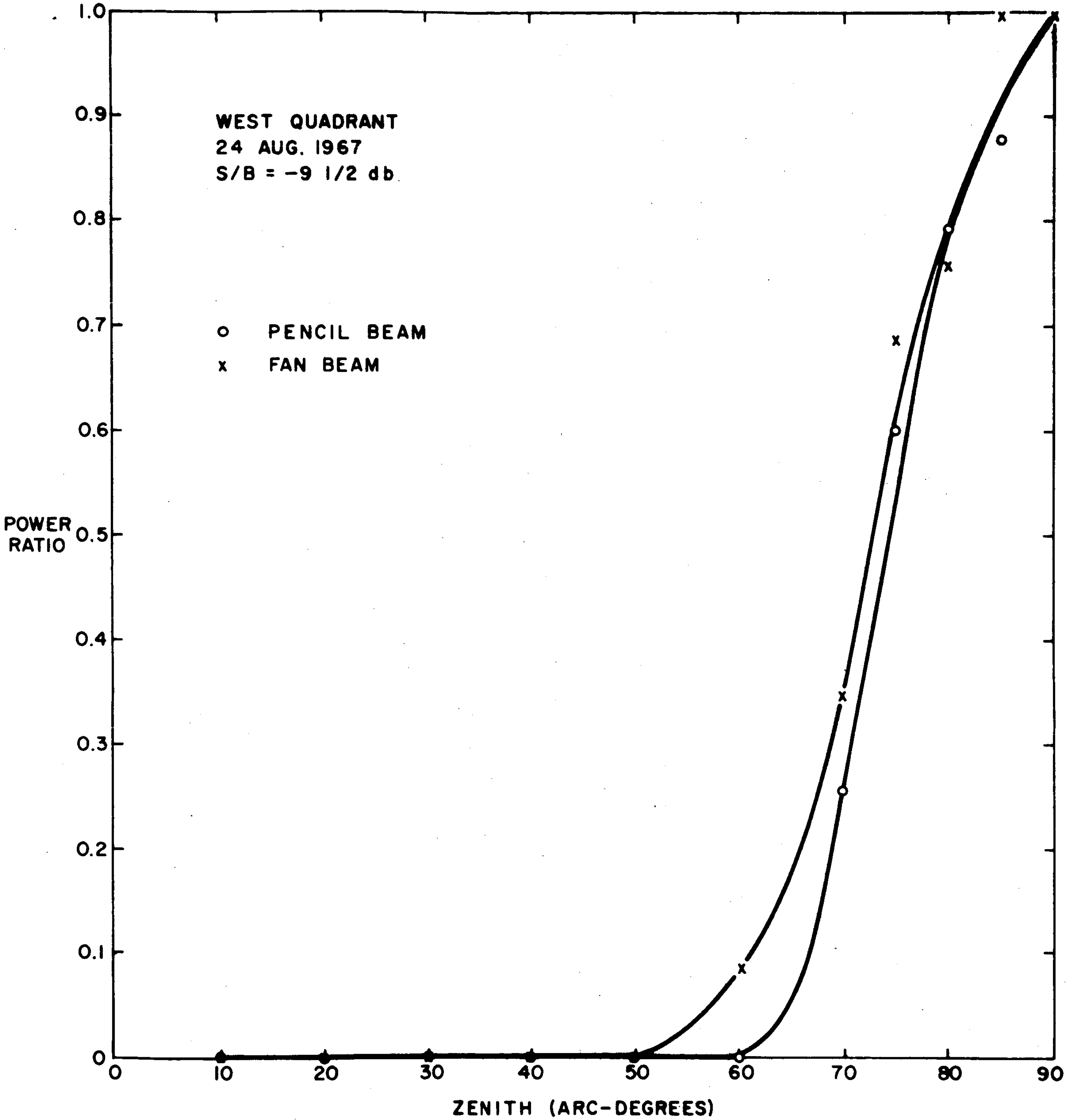

Figure 3-12 Measured Antenna Pattern

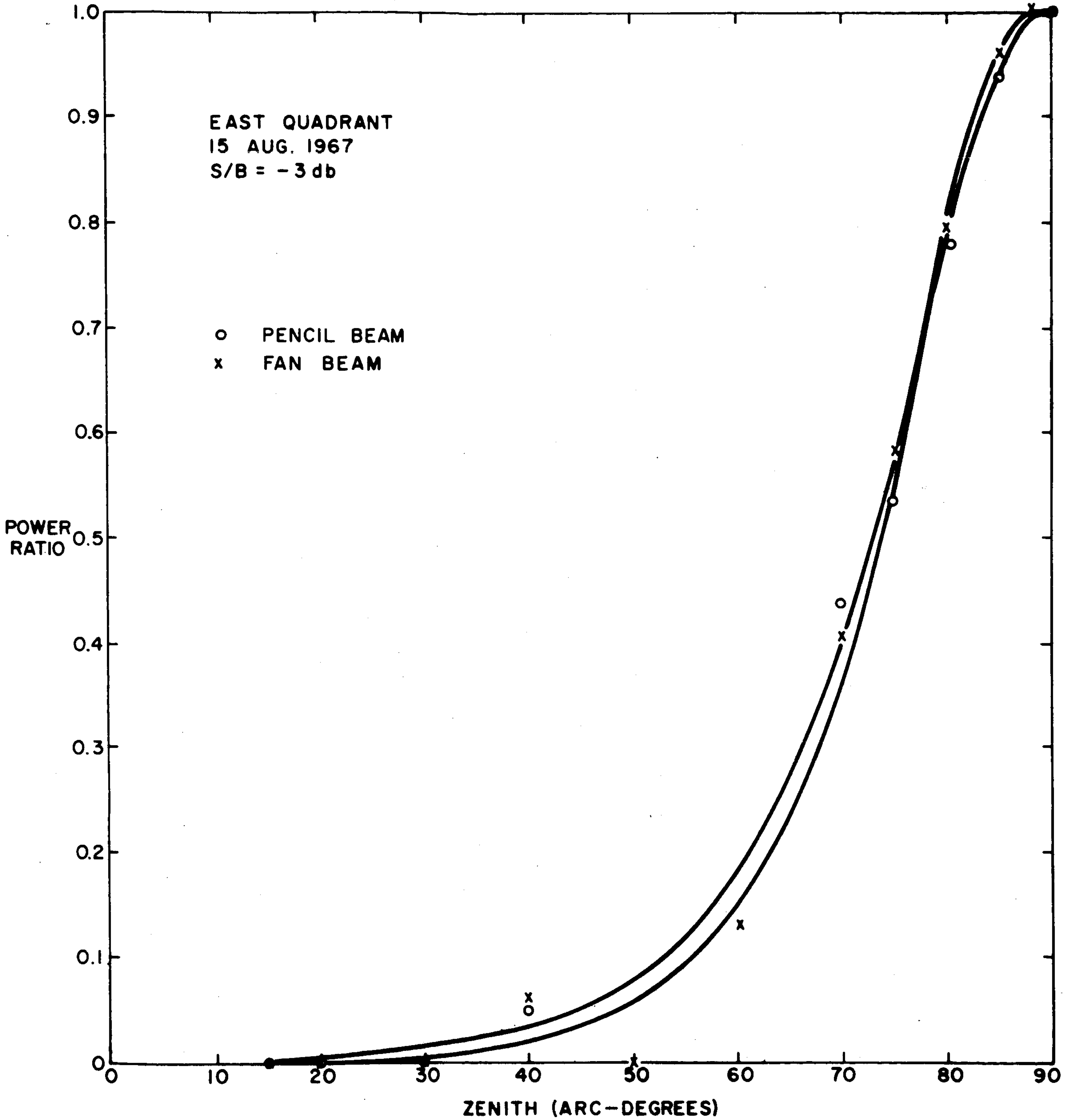

Figure 3-13 Measured Antenna Pattern

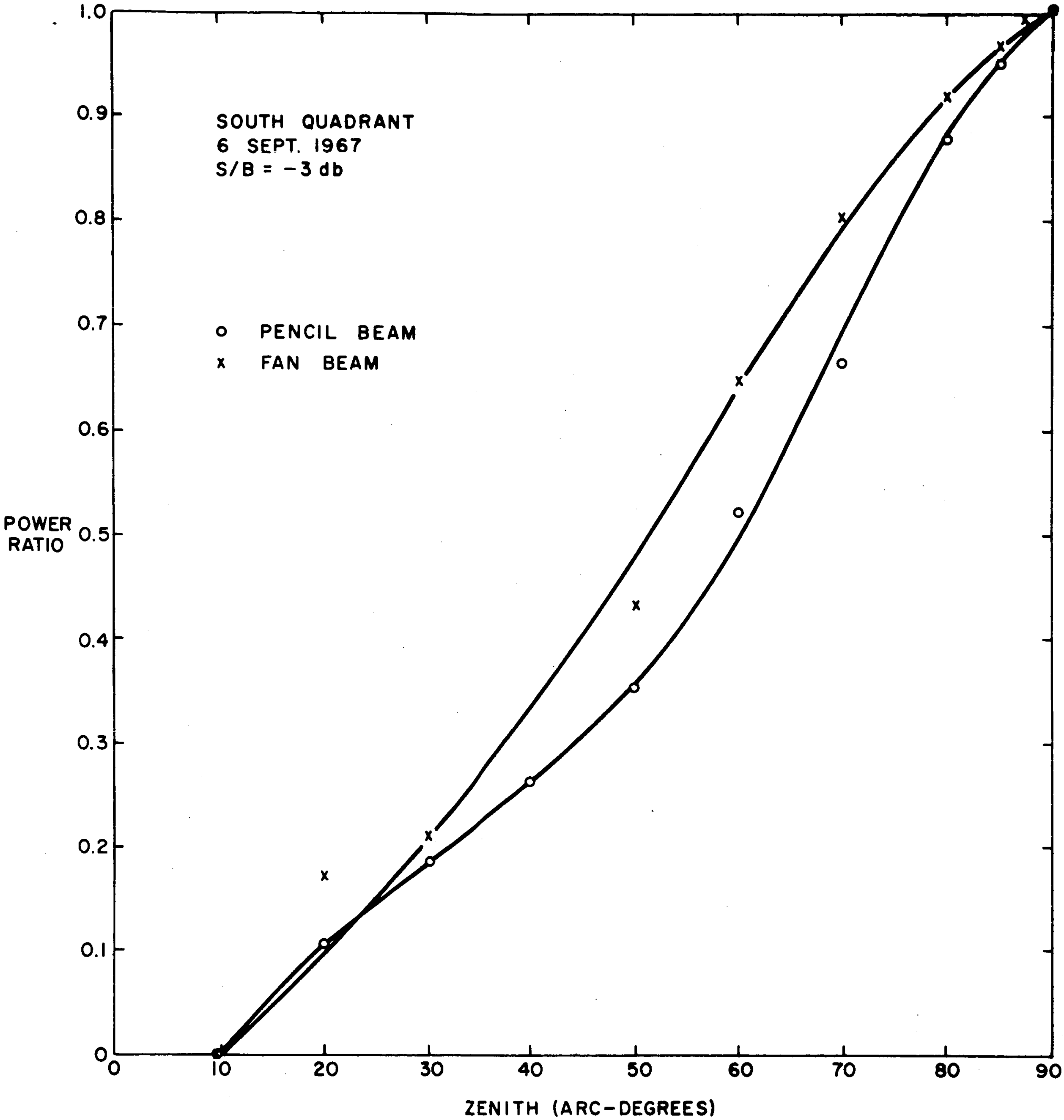

Figure 3-14 Measured Antenna Pattern

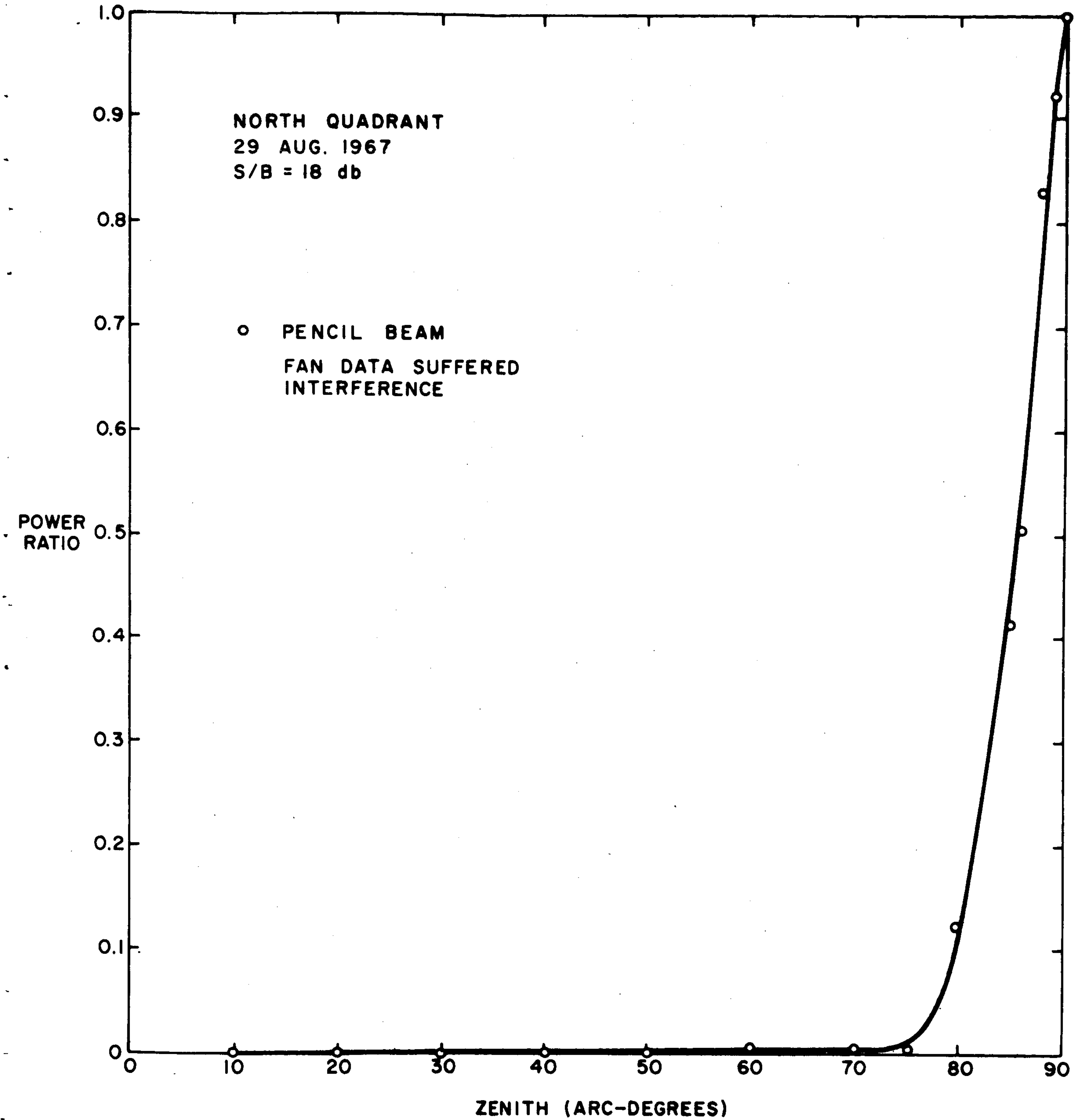

Figure 3-15 Measured Antenna Pattern

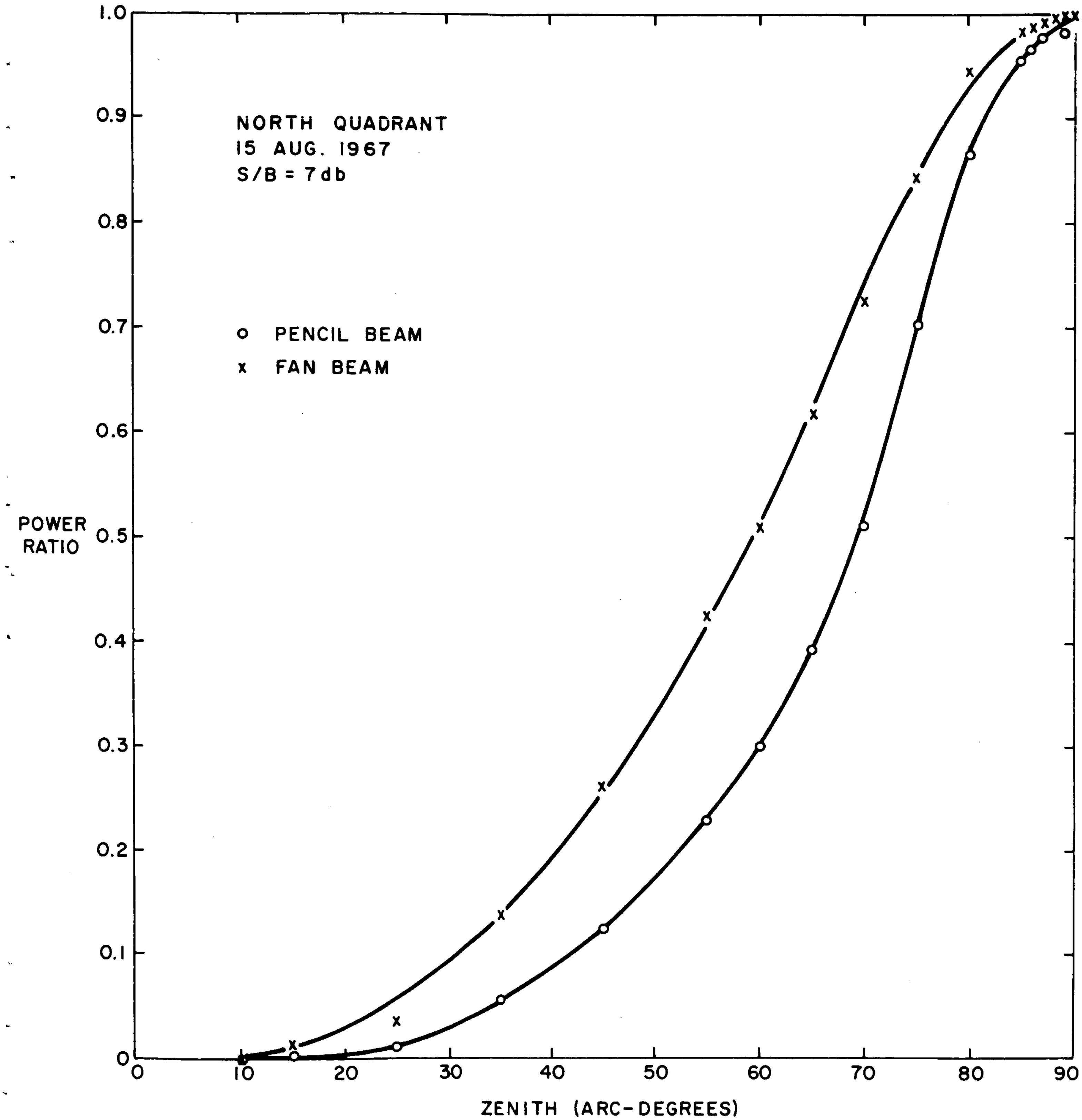

Figure 3-16 Measured Antenna Pattern

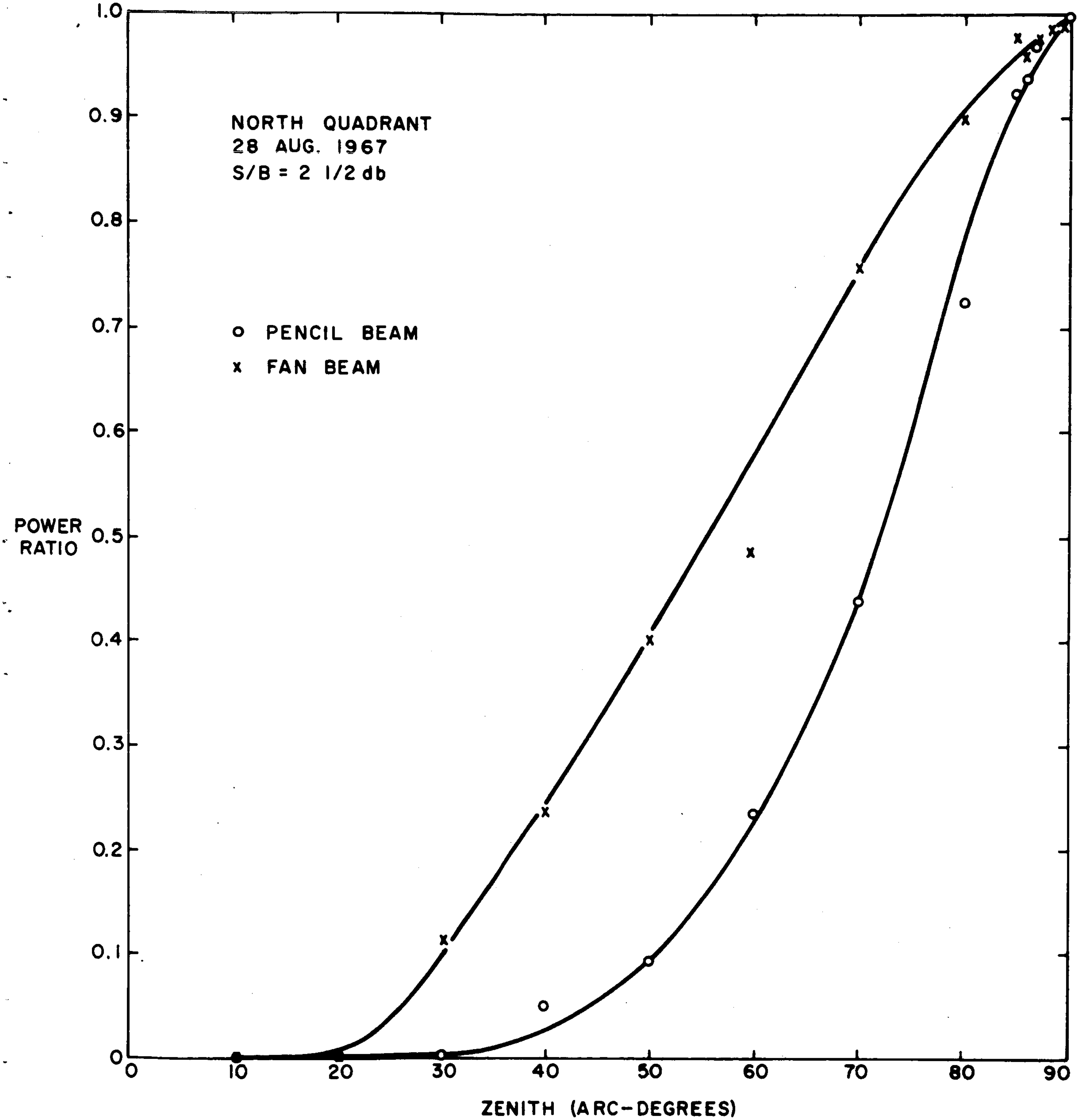

Figure 3-17 Measured Antenna Pattern

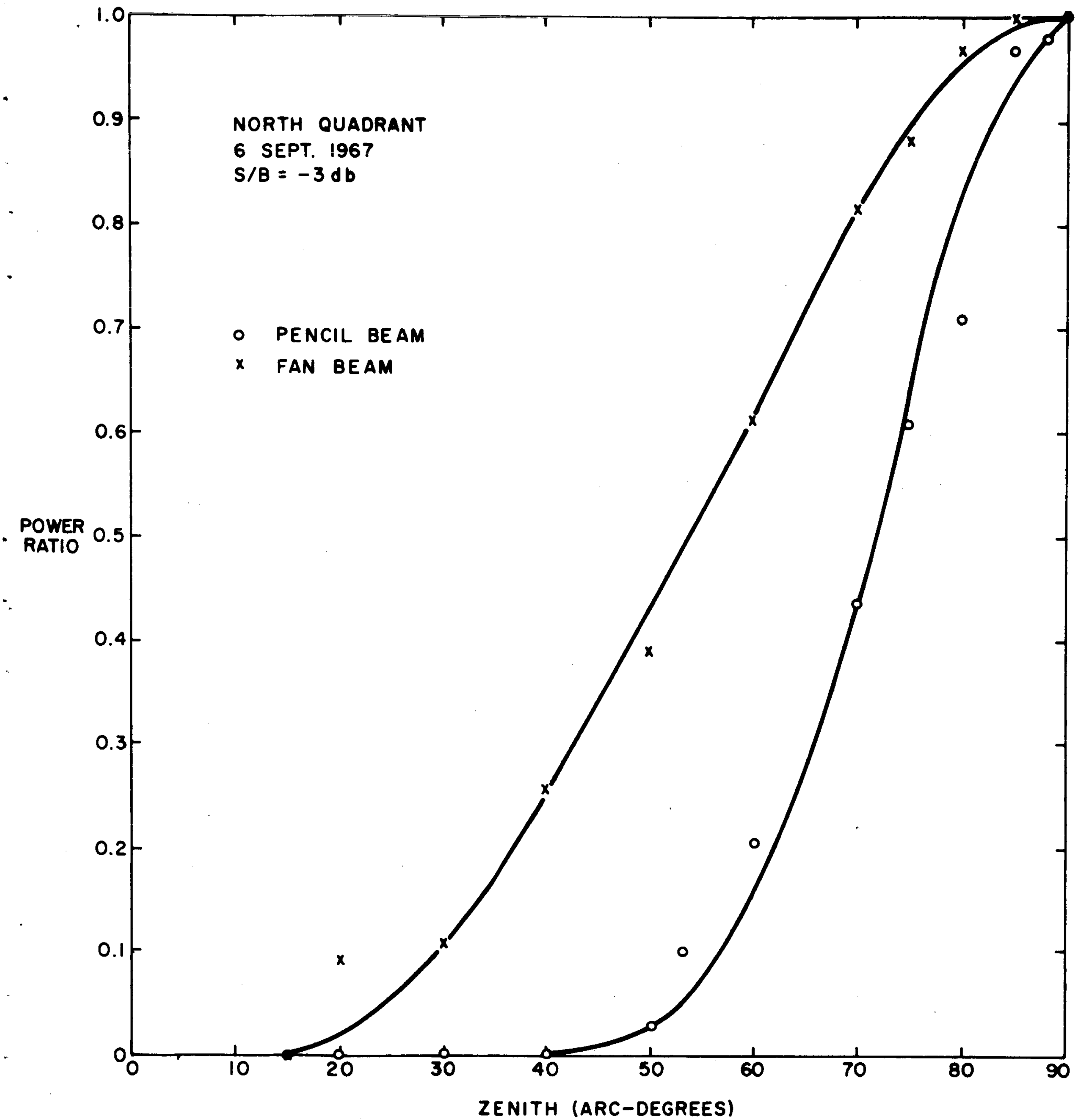

Figure 3-18 Measured Antenna Pattern

The low source-to-background ratio patterns are shown in Figures 3-11 to 3-14 and Figure 3-18. For these patterns, the antennas were connected directly to the hybrid outputs so that full cosmic noise was present in the receivers. The source-to-background ratio for each of the patterns was determined from the signal (sum) pattern. Thus, the ratio, S/B, is defined as:

$$S/B = 10 \log_{10} \left[\frac{(Ta)px}{(Ta)cn}\right]_{sum}$$

and for 0 db S/B, the signal (sum) pattern receiver output deflection (square law) will double when the source is ignited at zenith. Again, corrections for changing source distance are included in these patterns. The angular resolution as a function of S/B ratio is shown in Figure 3-19.

The low S/B ratio patterns were made between 0000 and 0600 local time to minimize effects of interference. The error bars in the patterns are due primarily to the variance of the noise being measured. A sample of the raw data from the chart recorder is shown in Figure 3-20. The printed paper tape data was used for evaluation.

3.3 System Calibration

System calibration consists primarily of three steps:

1. Primary calibration of the transfer calibration equipment
2. Linearity tests of pattern detectors
3. Radiometer measurements of reference and signal patterns

The details of these calibration steps will be discussed in the sections to follow.

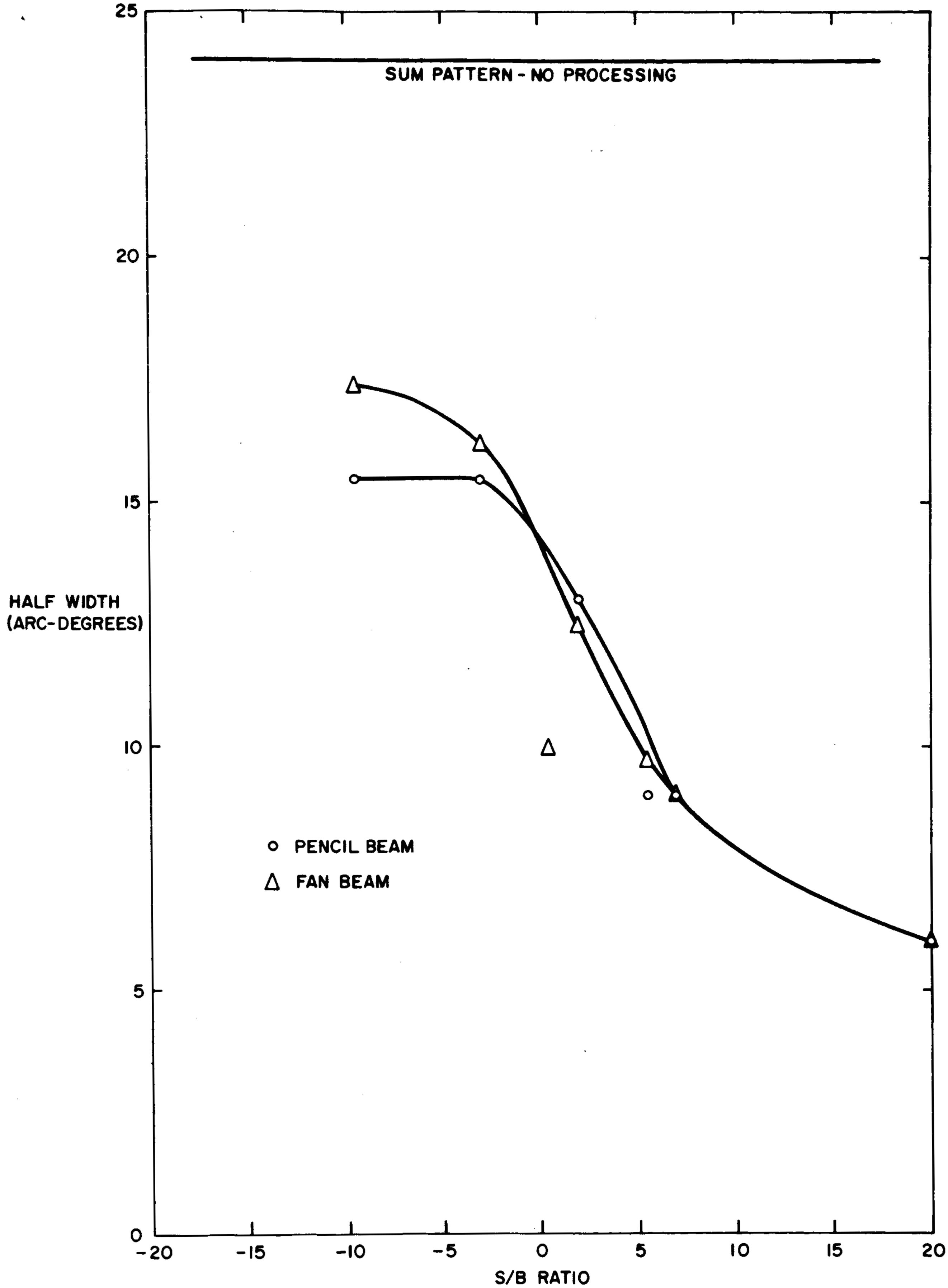

Figure 3-19 Angular Resolution as Function of S/B Ratio

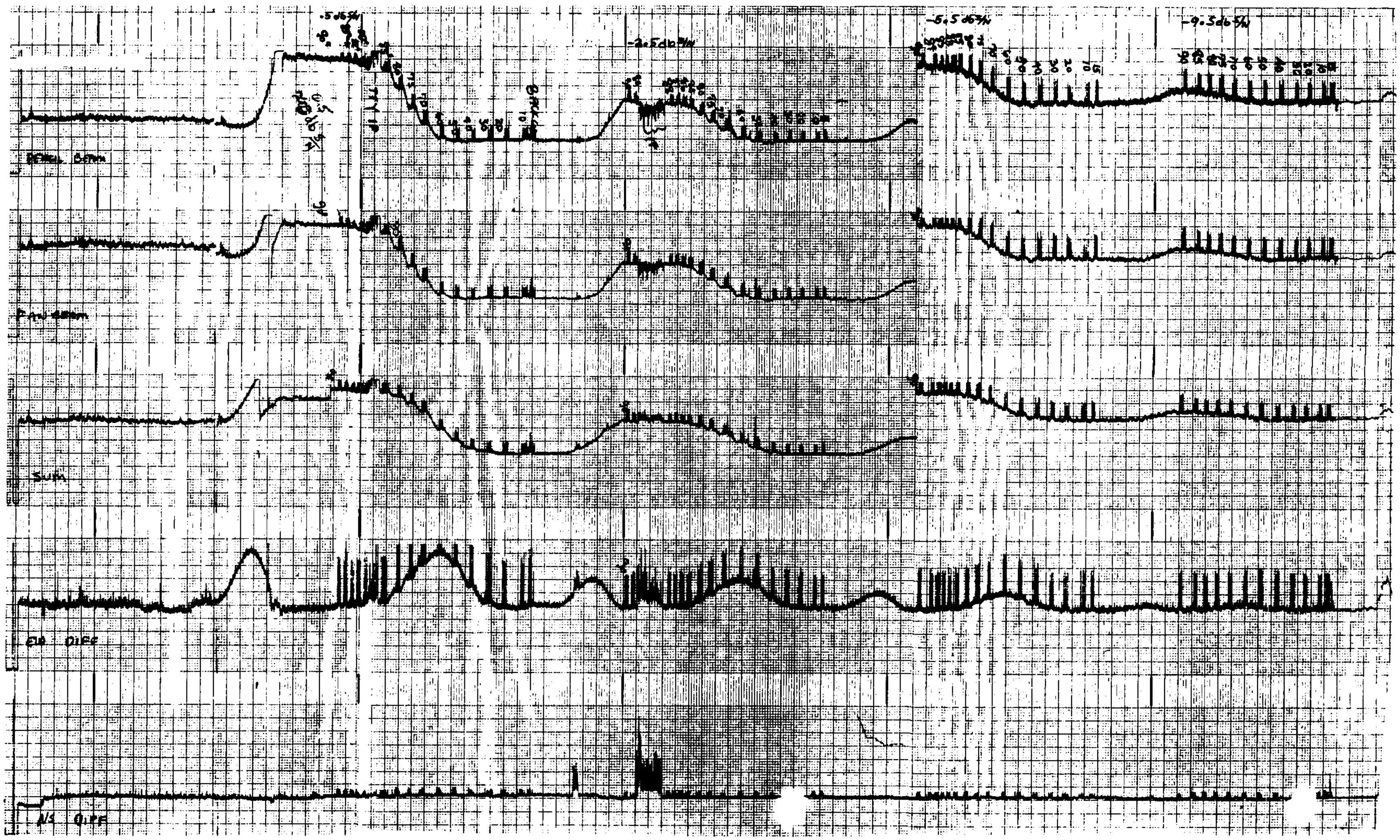

Figure 3-20 Sample of Raw Data

3.3.1 Primary Calibration

The primary calibration of the transfer calibration equipment was divided into two steps. First, the outputs of the six noise generators were calibrated as a function of control voltage (see Figure 2-7). A specially designed comparison radiometer was utilized for this calibration at 22 MHz which has a relative accuracy of ± 0.01 db and an absolute accuracy of ~ 0.07 db. The operation of this radiometer has been described elsewhere (Hartai, 1967). The results of the noise generator calibration are shown in Figure 3-21.

The second step consisted of measuring the transfer function of the noise synthesizing circuitry shown in Figure 2-9. This was accomplished by measuring individually the attenuators which make up the equipment and by measuring the noise output from the signal and reference channels due to each noise generator using a comparison radiometer.

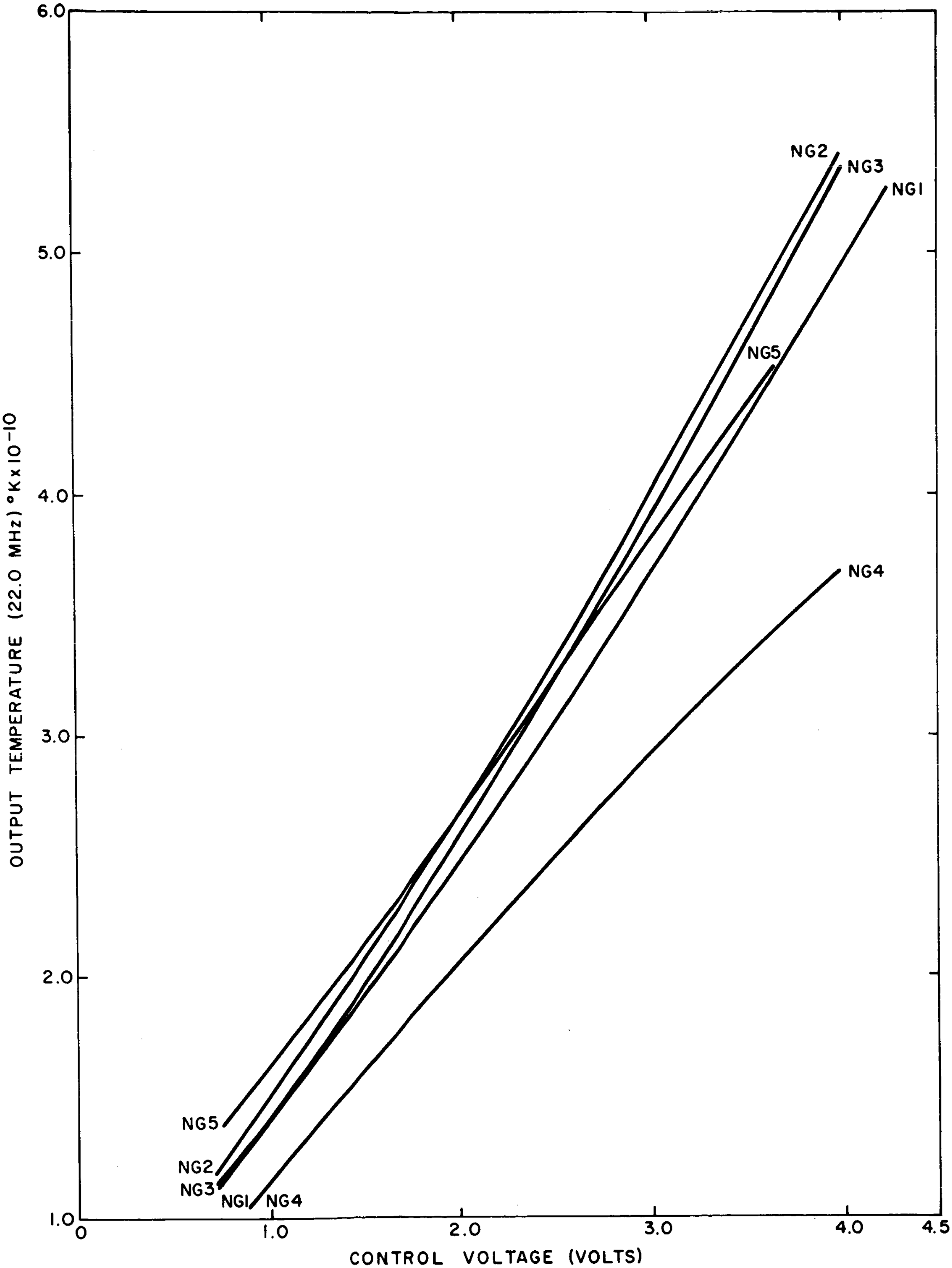

Figure 3-21 Noise Generator Calibration

4.0 Observations

Following the installation and initial tuning of the antennas, receivers, and processor, observations of the background cosmic noise were obtained and compared with a 10 arc-degree pencil beam from a conventional array of 64 dipole elements. Considerable problems with man-made solar interference were experienced due to the current upswing of solar activity and the accompanying increase in ionospheric critical frequency (f_oF_2). The interference increased very markedly over the last year since the preliminary measurements were made.

4.1 Data from the 4-Dipole Array

The 4-dipole array observations were made by allowing the earth's rotation to carry the antenna pattern, which was kept in the local meridian, through the complete range of right ascension every 24 hours. The declination of the beam was controlled by adding additional transmission line delay in the north or south antenna feeder as appropriate. Observations were concentrated on declinations of +40° and +58° corresponding to the radio sources Cygnus A and Cassiopeia A respectively. The beam of the 64-element phased array was similarly steered in declination with the addition of seven appropriate sections of transmission line. A Ryle-Vonberg receiver was used with the 64-element array.

The chart record of a typical 24 hour observational period is shown in Figure 4-1. In addition to the pencil beam and fan beam outputs from the processor, Figure 4-1 also shows the

Figure 4-1 Chart Record of T

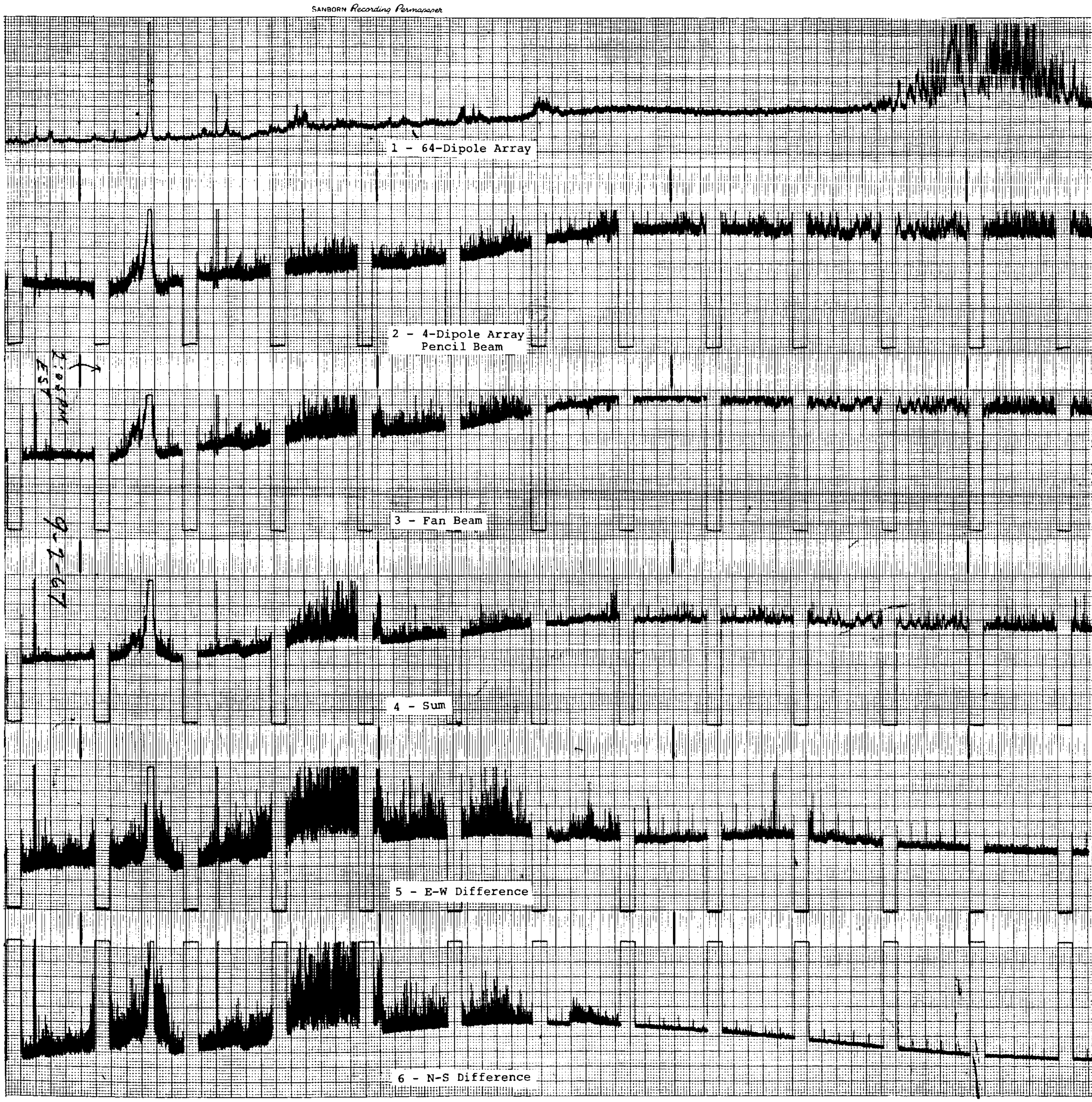

ypical 24 Hour Observation

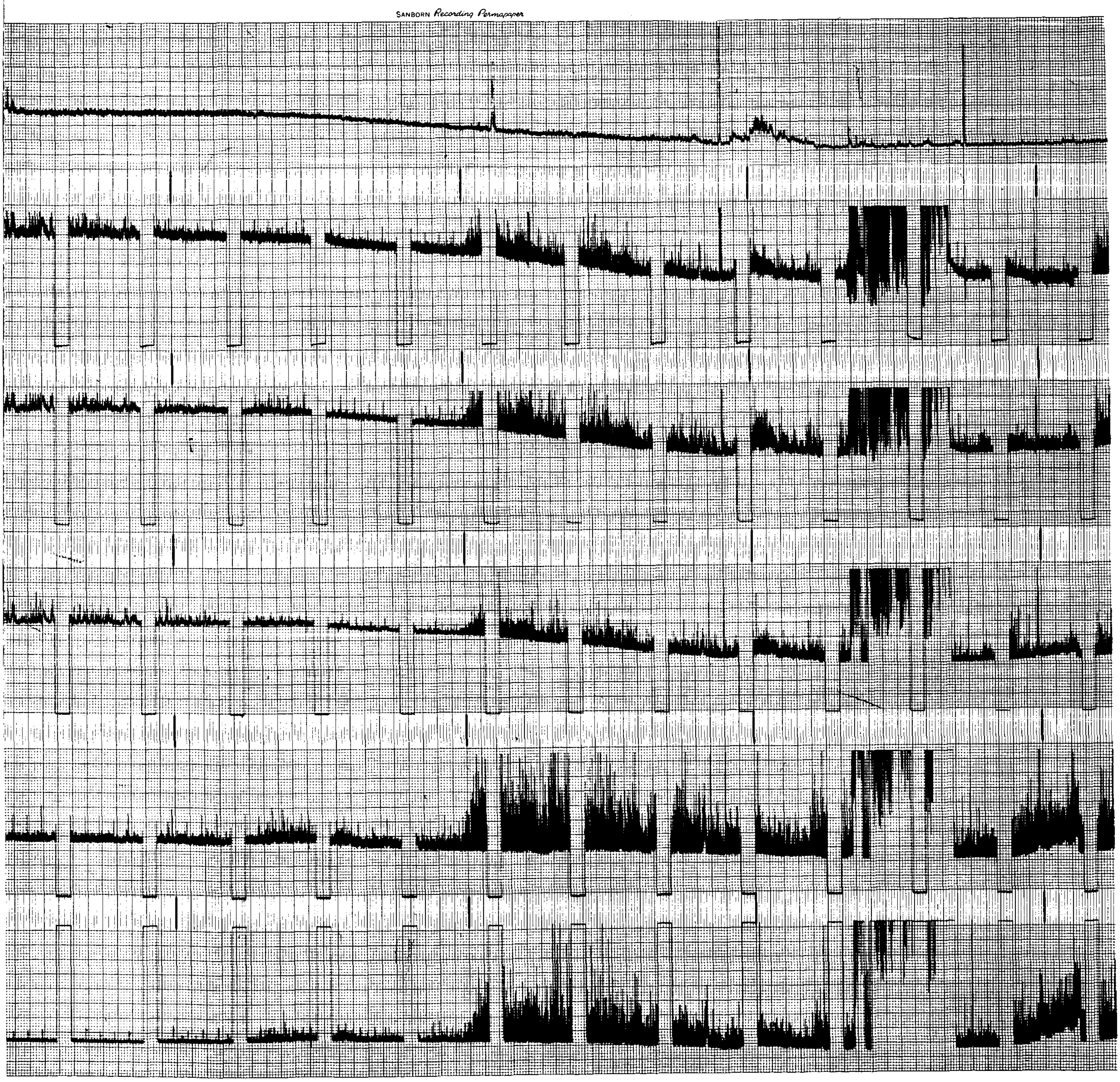

58-2

detected total power from the signal (Σ) and two reference (Δ) patterns. The outputs of the various receivers and the noise generators were also recorded on printed paper tape. The data analysis was primarily from the printed paper tape, however, continual reference was made to the chart records to clarify periods of calibration and interference.

The paper tape records were normalized to the calibration and plotted vs. the right ascension of the local meridian. Obvious interference points were rejected. Points of suspected interference were checked against the chart records. Averages of the raw data were made and corrections applied for receiver linearity.

An additional check on the main beam size was made by observing the upper transit of the source Cassiopeia A. In particular, the amplitudes of scintillations between the two antennas were compared. An example of this data is shown in Figure 4-2.

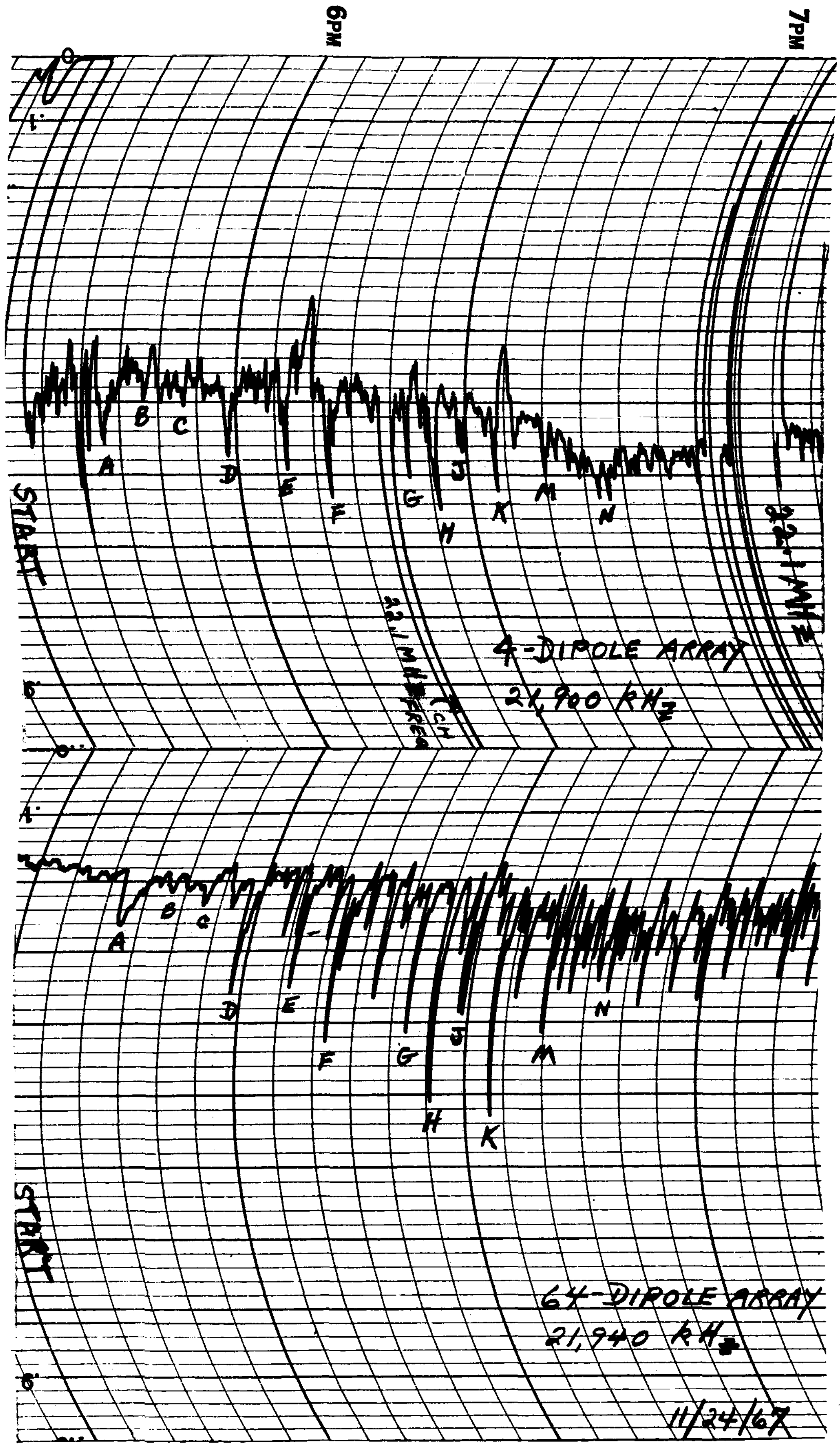

Figure 4-2 Cassiopeia A Amplitude of Scintillations Comparison for 4 and 64 Dipoles

5.0 Conclusions and Recommendations

The primary conclusion of the feasibility study is that the current system forms the desired 10 arc-degree pencil beam at positive signal-to-noise ratios. For zero and negative signal-to-noise ratios, the beam degrades to approximately a 30 arc-degree beam. This behavior, shown in Figure 3-19 for the pattern measurements, was substantiated by the cosmic noise observations. It is the opinion of these investigators that a portion of this non-linear behavior and in particular the bad side-lobes can be eliminated with better diode devices in the processor gates. The use of the processor system for background studies is not currently feasible. If better solid-state devices can be developed, however, the high-level negative side-lobes observed can be significantly reduced.

The real use of the processor system, however, is for observing high level sporadic sources. Aperture synthesis and derivative techniques requiring time stationary sources are obviously not applicable to the observations of such sources. In particular, the use of the processor system for determining the origin of certain high intensity burst radiation from such solar system sources as the Sun, Jupiter, or the Earth would be an invaluable complement to interferometric and spectral systems on any future Radio Astronomy Observatory. Specifically, the knowledge of the point of origin of a burst of radiation would provide an independent double check on the phase-path lengths and base-line orientation of an aperture synthesis or other interferometer system.